Department of Precision and Microsystems Engineering

Design and Fabrication of a Dielectric Elastomer Actuator for Organ-on-Chips Platforms

Chuqian Zhang

Report no : 2019.033
Coach : dr. M. Mastrangeli dr. M. K. Ghatkesar
Professor : dr. ir. M. Tichem
Specialisation : Micro and Nano Engineering
Type of report : Thesis
Date : 19 September 2019

Design and fabrication of a dielectric elastomer actuator for Organ-on-Chips platforms

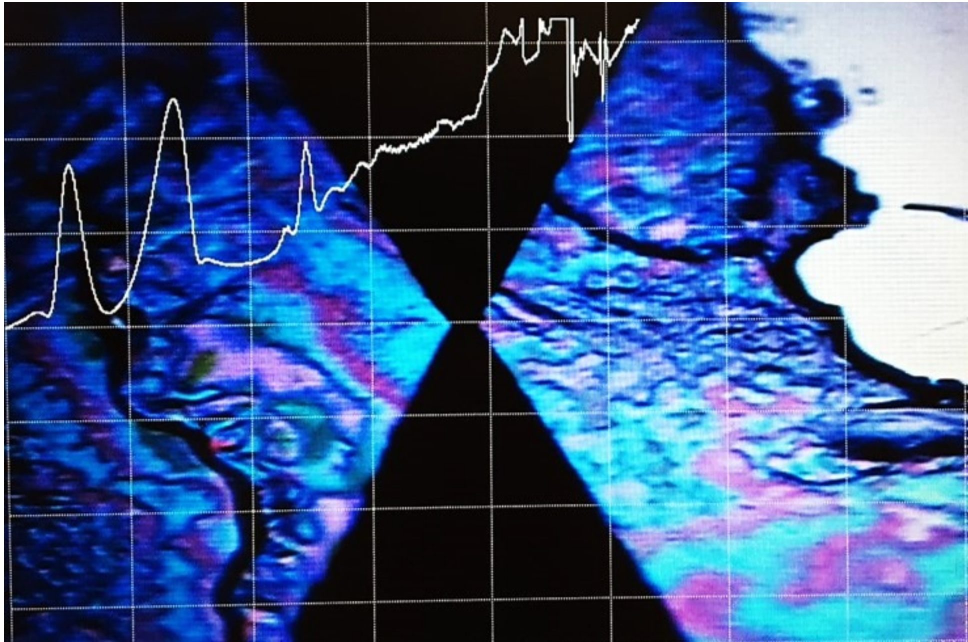

Chuqian Zhang

in partial fulfilment of the requirements for the degree of

Master of Science
in Mechanical Engineering

at Delft University of Technology,
to be defended publicly on Thursday September 26, 2019 at 10:00AM

Thesis committee:
dr. ir. M. Tichem (Chair), TU Delft
dr. M. Mastrangeli (Supervisor), TU Delft
dr. M. k. Ghatkesar (Co-supervisor), TU Delft
prof. dr. P. J. French (external member), TU Delft

Copyright © 2019 by C.Zhang
An electronic version of this dissertation is available at
http://repository.tudelft.nl/.

Contents

Abstract vii

Acknowledgements ix

1 Background 1

1.1 Time Has Come For Organ-On-Chips 2
1.2 Cytostretch, an Organ-on-Chip Platform 3
1.3 Problem identification 4
1.4 Outline of the Thesis 4
References 5

2 Literature review 7

2.1 Basic Principles of Polymer-Based Actuator Design 8
2.1.1 Pneumatic Actuators 8
2.1.2 Electrically Responsive Actuators 10
2.1.3 Evaluation and Selection 15
2.2 Research Goals and Bottlenecks 16
References 17

3 Design and Fabrication of Dielectric Elastomer Actuators for Organ-on-Chip Platforms 19

3.1 Introduction 20
3.2 Design 20
3.3 Material Selection 22
3.4 Finite Element Analysis 26
3.5 Fabrication 29
3.6 Results 30
3.6.1 PDMS-PI adhesion 30
3.6.2 PI depositing and curing 31
3.6.3 TiN depositing and patterning 32
3.6.4 PDMS etching 34
3.7 Discussion 34
3.8 Conclusion 36
3.9 Outlook 36
References 39

4 Reflection 41

A appendix A 45

A.1 Basic Principles of Polymer-Based Actuator Design 45
A.1.1 Thermal-responsive hydrogels 45

A.1.2 Magnetic actuated dynamic surfaces 47
A.1.3 Mechanical actuators 49
A.1.4 Photothermal actuators 50
A.1.5 Chemical sensitive dynamic hydrogels. 50
A.2 Concept Evaluation forms 52
A.3 Lumped PDMS model calculation 54
A.4 Flowchart 55
A.5 PDMS spin coating thickness configuration. 68
A.6 PI Koyo oven curing recipe 70
References 71

Abstract

Cell behaviour *in vitro* can be regulated by mechanical stimulation. Cytostretch is an Organ-on-Chip (OOC) platform that allows cyclic stretching tissue in culture. Its pneumatic actuation can hinder it from microfluidic systems integration. A dielectric elastomer actuator (DEA) was developed and fabricated in this thesis for Cytostretch as an alternative actuation method. The DEA consists of a suspended polymer membrane sandwiched between electrodes, which can induce out-of-plane motion when a voltage is applied. The functionality of the design was proved in numerical analysis. A complete process flow was developed and partly implemented for the wafer-scale microfabrication of this innovative actuator. The top electrodes of the device were fabricated by depositing and patterning titanium nitride with stress buffering layers. The quality of the electrodes was examined and wrinkles were found at corners of certain etching patterns. The angle of the corner and spacing between corners are proposed to be two factors influencing the wrinkle formation. This work paves the way to the successful integration of DEAs for mechanical stimulation of cell tissues within OOC platforms.

ACKNOWLEDGEMENTS

I would first like to express my deepest gratitude to my supervisors, Massimo Mastrangeli and Murali K Ghatkesar. Thank you for guiding me and giving me valuable suggestions since the very beginning of my thesis. I was always motivated every time after we had a meeting. I feel lucky that I have you as my supervisors.

Dear Massimo, I am really appreciated that I was given the opportunity to implement my idea and try to make it real by myself in the cleanroom. Thank you for answering my questions and gave me chocolate once when I just randomly jumped into your office. I am sorry that I sent you emails in the late evening or on weekends several times (and you replied). I remembered a lot of tiny stories. For example, you asked if I found a way to go home after the ECTM annual party (in a location close to nowhere) because you knew I did not take my bike that day. You allowed me to have 24h access in the cleanroom but also told me not to deprive my sleep. You sent me an email to encourage me when you heard I broke my wafer. These things are tiny but I am really grateful and always happy when I think about them.

Dear Murali, I would like to thank you for always asking me critical questions during meetings. Questions are burning for sure but it helped me a lot to know where is the missing part of my project (and my logic) and evaluate it from a different perspective. I like the discussion about the book 'Factfulness' and your white rhombus shape sweets (I still don't remember the name). Thank you for taking me to the 'Life' conference and laughed when I said the color of the wine was similar to the photoresist. Our small chatting about doing PhD, work and life can always give me new inspiration. We talked about my ukulele several times so maybe in future I can eventually find a chance to perform you a short song.

A lot of thanks to the people in EKL cleanroom and special thanks goes to Tom, Johannes, Hitham, Silvana and Mario. Thank you for sharing your years of working experience with me and giving hints to my problems. It might be common knowledge to you but you saved my process totally many times. Dear Paolo, I like your hat (or hats) and you are a man with a great taste of style (and jokes).

I would like to thank lots of help, laughter and friendship I got from the PhDs in my group. Dear Hande and Milica, we have more people in the gang now but we were the three that started everything together in the beginning. I love the guessing game we played when waiting for machines in the cleanroom training and I hope you like the food (like the hotpot and sushi) I made. Dear Milica, I still owe you the chocolate mochi debt. Dear Hande, please share with me when you have new super cool tattoo ideas, like we did before in the workshop. Dear Paul, we should have another drink and discuss the backup plan of a farm if things are not working. Dear Safoora, thank you for bringing me the beautiful plant. It is still very healthy and green.

Special thanks goes to the master students that I was so lucky to know. Dear Raghutham ramesha, lord Mauricio, Suus (and your wafer plant), sweet Bart and Caitlin, we defi-

nitely should have the board game night again with team breaking strategy. Dear Arun and Nimit, it was a pleasure to play pool with you. All I need is to try hard and something will happen eventually. Dear Jiarui, thanks a lot for being my buddy all the time in the cleanroom. It would be so boring and quiet without you.

Thanks to my friends here and back home. Some of you might not understand the content of my thesis but I know you always understand and support me. I will share my joy with you for sure, just like we shared all the gossip and secrets. Dear Yi, I want to give you a lot of energy here to support you working for thesis. I know you had a lot of hard times but I believe the power in you. A special thanks goes to my roommate Gaia for encouraging me all the time, especially when I told you I had a hundred ways of landing on the sofa and procrastinate there. I could not wait to go to the aquarium with you after my defense.

Finally, I would like to thank my parents. Seldom we say it out but here is the perfect chance: I love you and I am happy to make you proud. Your unconditional love is my shelter and armor to explore the world. I am not afraid of anything as long as I think of you.

1

BACKGROUND

1

1.1. TIME HAS COME FOR ORGAN-ON-CHIPS

Novel reliable technologies have been expected from the pharmaceutical industry to solve its current dilemma. Since the 1970s, the cost invested for Research and Development (R&D) by the pharmaceutical industry has increased exponentially [1]. However, the number of compounds entering the market has not increased respectively, leading to higher development costs per drug [2]. The decreasing of the drug development success rate during testings [2] can be one of the reasons.

Conventional testing methods used in drug development, mostly in the preclinical stage, such as cell culture using petri dishes and animal models have their limitations. The 2D structure of the cell culture cannot sufficiently replicate the 3D dynamic environment *in vivo*. Due to the difference between human and animal physiology, animal models may not provide enough insights into human responses to the drugs. Certain existing drugs in the market have to be withdrawn mainly because of cardiac and liver toxicity which were not predicted in preclinical stage [3]. Therefore, new alternatives are expected to understand better the mechanism of drugs, corresponding cell behaviours and organ level interactions, improving preclinical testing accuracy and efficiency.

Organ-on-Chips(OOCs), microfluidic devices designed to simulate physiological functions of tissue and organs [4], might be the solution. The word 'chip' refers to the microfabrication methods applied originally in the electronics industry [5]. Most of current OOCs are mimicking one specific functional unit of an organ, such as liver [6], lung [7], kidney [8], heart [9] and gut [10]. Researchers have also developed OOCs reflecting tissue-tissue interfaces such as blood-brain barrier [11]. Eventually a 'human-on-a-chip' [12] system is expected by integrating different organ-level functional units.

Polydimethylsiloxane (PDMS) is one of the most common materials used in OOCs devices. The polymerization of PDMS requires a mixture of two components, a siloxane oligomer base and a curing agent. The mechanical properties of the PDMS can be tuned by altering the mixing ratio, yet usually the ratio 10:1 (base:curing agent) is adopted. PDMS is suitable for biological applications due to its optical transparency [3], biocompatibility and permeability [13]. In addition, its mechanical property, especially Young's modulus, make it a compliant soft material potentially being the ideal substrate for complex tissue surfaces [14].

Although PDMS is widely applied in microfluidic devices, it certainly has limitations. The porosity of PDMS allows small molecules such as chemokines and cytokines to diffuse or bind into the polymer. This may cause the difficulty of drug dose control and estimation during certain experiments [15]. For this thesis in particular, the high thermal expansion factor of PDMS, its hydrophobicity and incompatibility to conventional lithography have led to fabrication difficulties, which will be discussed in chapter 3.

OOCs and their promising possible applications have attracted more attention from academia and industry. However, there is still a long way before they mature and reach a mainstream. Although several OOCs products are commercially available, they are not integrated into the research and development process from pharma companies [16]. More challenges are expected in future, yet the light of this novel technologies has been ignited. It is still early to predict but expectations are high that a time for OOCs will come.

1.2. CYTOSTRETCH, AN ORGAN-ON-CHIP PLATFORM

When designing OOCs to mimic crucial attributes of physiological conditions, one should consider mechanical forces, displacement and strain that cells normally experience *in vivo*. For example, cells in the musculoskeletal system are under weight bearing and stresses caused by locomotion [17], and cells on intestinal barrier are experiencing periodic contractions induced by muscular layers of the bowel [18]. Mechanical stimulation plays an important role in various cell stages such as growth, differentiation, migration and apoptosis ('Programmed cell death') [19]. An OOC device establishing a dynamic environment with specific mechanical properties would be valuable to study tissue behaviour *in vitro*.

Cytostretch [20] is an OOC platform that allows cyclic mechanical stretching on the tissue in culture. The basic structure is a suspended PDMS membrane on a silicon substrate (Figure1.1(a) [20]). Cytostretch platform was originally developed for a Heart-on-Chip model [21]. When connected to an external pumping system, the PDMS membrane can be actuated pneumatically (Figure 1.2 [20]).

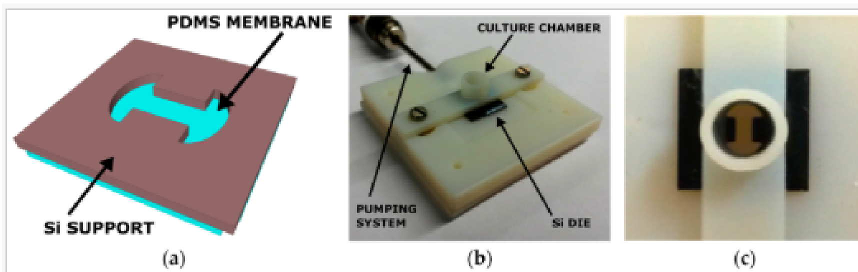

Figure 1.1: (a)Back view sketch of the Cytostretch; (b) 3D-printed holder with a pumping system for Cytostretch; (c) Top view of the Cytostretch with the holder [20]

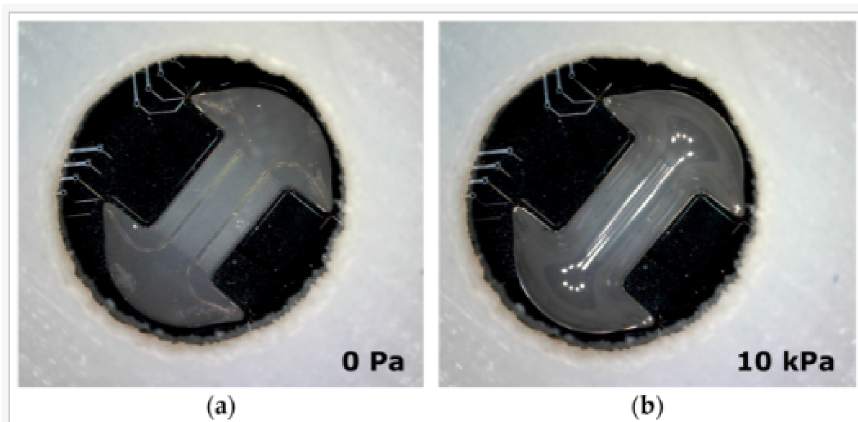

Figure 1.2: (a) Cytostretch at relaxed state; (b) Cytostretch inflated with 10kPa from the back of the membrane [20]

Compared to other OOCs devices, Cytostretch has an advantage that it can be customized and integrated into various applications. By adding or altering certain features during fabrication, it can be equipped with through-membrane pores, microgrooves [20], stretchable microelectrode array (MEA) [21] and other sensors [22] [23]. Preliminary biological tests have been made to assess the functionality and biocompatibility of Cytostretch. A visible impact has been found on the cultured cardiac monolayer after applying cyclic stretch for 5 days on Cytostretch [24].

1.3. PROBLEM IDENTIFICATION

It is certain that Cytostretch has been elaborately designed, developed, fabricated and tested, yet there is still space left for further development. One of the important limitations is that it did not have integrated microfluidic systems. Although the PDMS membrane can be fabricated with through-membrane pores, lacking the integrated microfluidic channels can hinder the applications of cross membrane communications and compounds interchange. In addition, cells can only be cultured on the top side of the PDMS membrane since the space underneath is designed for the pneumatically actuated chamber. Interfaces study of two cell types is not applicable to current Cytostretch platform.

Besides the limitation of microfluidic systems, current actuation method of Cytostretch was not suitable for independent parallel control. A multiwell plate has been developed for Cytostretch [25], yet cyclic stretching cannot be controlled separately for each well unless multiple pumping systems are applied. Finding solutions to the limitations of Cytostretch as discussed above was the original motivation and goal of this thesis. It has been proposed that if a more compact actuation design can be applied to Cytostretch, the space originally saved for the air chamber can be used for microfluidic channels. Independent parallel control might be achievable as well. More details will be discussed later in chapter 2 and chapter 3, yet this is where the initial ideas and inspirations started.

1.4. OUTLINE OF THE THESIS

The goal of this thesis is to develop a polymer-based actuator for OOC platforms. In particular, this thesis aims at designing an actuator that can induce out-of-plane motion to provide an alternative actuation method for Cytostretch. In order to achieve this, the full fabrication process flow was defined with critical steps tested. There are four chapters in this thesis. The first chapter introduction explains the motivation and goal of this thesis, followed by a small review in literature to provide essential background information in chapter 2. In these two chapters, the basic questions 'why this topic' and 'What to achieve' are answered.

Chapter 3 is the main chapter of this thesis. It presents the whole development flow of the thesis work. First how the DEA for Cytostretch is designed, then the simulation results to predict the functionality. The main focus will be addressed on the fabrication process, as also being one of the research goals, to find applicable steps for patterning TiN electrodes on soft substrate. The results will be discussed followed by an outlook of future possibilities. This chapter answers the question 'How to do it '.

Chapter 4 is a reflection on this thesis. This chapter focuses on the reasoning and

evaluations behind the project. After one year of working, what experienced was learned, what deviated from the plan and what could I improve next time.

REFERENCES

[1] O. Gassmann, A. Schuhmacher, M. von Zedtwitz, and G. Reepmeyer, *Leading Pharmaceutical Innovation* (Springer, 2018).

[2] J. A. DiMasi, H. G. Grabowski, and R. W. Hansen, *Innovation in the pharmaceutical industry: New estimates of R&D costs,* Journal of Health Economics **47**, 20 (2016).

[3] B. Zhang, A. Korolj, B. F. L. Lai, and M. Radisic, *Advances in organ-on-a-chip engineering,* Nature Reviews Materials **3**, 257 (2018).

[4] S. N. Bhatia and D. E. Ingber, *Microfluidic organs-on-chips,* Nature Biotechnology **32**, 760 (2014).

[5] K. Ronaldson-Bouchard and G. Vunjak-Novakovic, *Organs-on-a-Chip: A Fast Track for Engineered Human Tissues in Drug Development,* Cell Stem Cell **22**, 310 (2018).

[6] S. S. Bale, L. Vernetti, N. Senutovitch, R. Jindal, M. Hegde, A. Gough, W. J. McCarty, A. Bakan, A. Bhushan, T. Y. Shun, I. Golberg, R. DeBiasio, O. B. Usta, D. L. Taylor, and M. L. Yarmush, *In vitro platforms for evaluating liver toxicity,* Experimental Biology and Medicine **239**, 1180 (2014).

[7] D. Huh, B. D. Matthews, A. Mammoto, M. Montoya-Zavala, H. Y. Hsin, and D. E. Ingber, *Reconstituting Organ-Level Lung Functions on a Chip,* Science **328**, 1662 (2010).

[8] K.-J. Jang, A. P. Mehr, G. A. Hamilton, L. A. McPartlin, S. Chung, K.-Y. Suh, and D. E. Ingber, *Human kidney proximal tubule-on-a-chip for drug transport and nephrotoxicity assessment,* Integrative Biology **5**, 1119 (2013).

[9] A. Marsano, C. Conficconi, M. Lemme, P. Occhetta, E. Gaudiello, E. Votta, G. Cerino, A. Redaelli, and M. Rasponi, *Beating heart on a chip: a novel microfluidic platform to generate functional 3d cardiac microtissues,* Lab on a Chip **16**, 599 (2016).

[10] H. J. Kim, D. Huh, G. Hamilton, and D. E. Ingber, *Human gut-on-a-chip inhabited by microbial flora that experiences intestinal peristalsis-like motions and flow,* Lab on a Chip **12**, 2165 (2012).

[11] R. Booth and H. Kim, *Characterization of a microfluidic in vitro model of the blood-brain barrier (BBB),* Lab on a Chip **12**, 1784 (2012).

[12] U. Marx, H. Walles, S. Hoffmann, G. Lindner, R. Horland, F. Sonntag, U. Klotzbach, D. Sakharov, A. Tonevitsky, and R. Lauster, *'Human-on-a-chip' developments: a translational cutting-edge alternative to systemic safety assessment and efficiency evaluation of substances in laboratory animals and man?* Alternatives to laboratory animals: ATLA **40**, 235 (2012).

[13] A. Dietzel, *Microsystems for Pharmatechnology* (Springer, 2016).

[14] L. Guo, G. S. Guvanasen, X. Liu, C. Tuthill, T. R. Nichols, and S. P. DeWeerth, *A PDMS-Based Integrated Stretchable Microelectrode Array (isMEA) for Neural and Muscular Surface Interfacing,* IEEE Transactions on Biomedical Circuits and Systems **7**, 1 (2013).

[15] M. W. Toepke and D. J. Beebe, *PDMS absorption of small molecules and consequences in microfluidic applications,* Lab on a Chip **6**, 1484 (2006).

[16] M. Mastrangeli, S. Millet, t. O. Partners, and J. v. d. E.-v. Raaij, *Organ-on-Chip In Development:Towards a roadmap for Organs-on-Chip,* (2019), 10.20944/preprints201903.0031.v1.

[17] J. Kim and R. C. Hayward, *Mimicking dynamic in vivo environments with stimuli-responsive materials for cell culture,* Trends in Biotechnology **30**, 426 (2012).

[18] D. Cei, J. Costa, G. Gori, G. Frediani, C. Domenici, F. Carpi, and A. Ahluwalia, *A bioreactor with an electro-responsive elastomeric membrane for mimicking intestinal peristalsis,* Bioinspiration & Biomimetics **12**, 016001 (2017).

[19] D. D. Chan, W. S. Van Dyke, M. Bahls, S. D. Connell, P. Critser, J. E. Kelleher, M. A. Kramer, S. M. Pearce, S. Sharma, and C. P. Neu, *Mechanostasis in apoptosis and medicine,* Progress in Biophysics and Molecular Biology **106**, 517 (2011).

[20] N. Gaio, B. van Meer, W. Quirós Solano, L. Bergers, A. van de Stolpe, C. Mummery, P. M. Sarro, and R. Dekker, *Cytostretch, an Organ-on-Chip Platform,* Micromachines **7**, 120 (2016).

[21] S. K. Pakazad, A. Savov, A. v. d. Stolpe, and R. Dekker, *A novel stretchable micro-electrode array (SMEA) design for directional stretching of cells,* Journal of Micromechanics and Microengineering **24**, 034003 (2014).

[22] W. F. Quiros-Solano, N. Gaio, C. Silvestri, G. Pandraud, and P. M. Sarro, *Polymeric strain gauges as pressure sensors for microfabricated organ-on-chips,* in *2017 19th International Conference on Solid-State Sensors, Actuators and Microsystems (TRANSDUCERS)* (2017) pp. 1296–1299.

[23] R. Ponte, V. Giagka, and W. A. Serdijn, *Design and Custom Fabrication of a Smart Temperature Sensor for an Organ-on-a-chip Platform,* in *2018 IEEE Biomedical Circuits and Systems Conference (BioCAS)* (2018) pp. 1–4.

[24] N. Gaio, *Organ-on-Silicon,* (2019), 10.4233/uuid:ceba7976-a4b0-469e-bdd0-70f0a14dc275.

[25] N. Gaio, A. Waafi, M. L. H. Vlaming, E. Boschman, P. Dijkstra, P. Nacken, S. R. Braam, C. Boucsein, P. M. Sarro, and R. Dekker, *A multiwell plate Organ-on-Chip (OOC) device for in-vitro cell culture stimulation and monitoring,* in *2018 IEEE Micro Electro Mechanical Systems (MEMS)* (2018) pp. 314–317.

2

Literature review

2.1. BASIC PRINCIPLES OF POLYMER-BASED ACTUATOR DESIGN

As mentioned in Section 1.2, a new actuation method might be the solution to current limitations of Cytostretch. Design principles of polymer-based actuators for cell-on-chips or organ-on-chips devices will be investigated in this section. Multiple designs, applications or stimuli-responsive materials were categorized based on basic principles of physics. Examples will be described in each category as well as discussions about advantages and limitations. Since the principle of Dielectric Elastomer Actuators (DEAs) were selected and applied in the design for this thesis, it will be focused and discussed with more details in the following paragraphs. Due to the page limit, content discussing polymer-based actuators using thermal, magnetic, mechanical, chemical and optical principles can be found in Appendix A.1.

2.1.1. PNEUMATIC ACTUATORS

Principle

Polymer-based pneumatic actuators in general use pressure-controlled chambers to deform a membrane where the cells are cultured. The air chamber can be designed under the membrane like Cytostretch, from sides like 'lung-on-a-chip'[1] (Figure 2.1 [1]) or surrounding the membrane like 'intestine-on-a-chip' [2] (Figure 2.2 [2]). Mechanical stretching is applied to cells during the inflating and deflating processes of the chamber.

Applications

One of the most successful OOCs using pneumatic actuators is the 'lung-on-a-chip'[1]. As shown in Figure 2.1 [1], this device mimics the breathing movement of the lung by using vacuum chambers and simulates the environment with shear in blood. Further testing with epithelium and endothelium cultured on this device proved that cyclic stretching (10% at 0.2Hz) can induce cell alignment [1]. When bloodborne immune cells were incorporated in the fluid, pulmonary inflammation was demonstrated successfully, proving that this OOC performed integrated organ-level responses [1].

Apart from the example introduced above, there are many OOCs chose to actuate the device using pneumatic pumps, for example, 'Heart-on-a-chip' to culture functional cardiac tissues [3] and 'gut-on-a-chip' [4] with a similar structure to previous 'lung-on-a-chip'. During the whole literature study period, it has been found that pneumatic actuators were relatively maturely developed and integrated in OOC products in the market.

Advantages and limitations

In general, polymer-based pneumatic actuators have simple structures that can be fabricated easily. The mechanical load and frequency applied to cells can be tuned by applying different pressure. Since OOCs and human tissues normally require the actuation frequency between 0.1-5Hz, the response time of pneumatic actuators is sufficient. Furthermore, one essential advantage is that pneumatic actuators have a relatively long lifetime. No report of breaking down was found during the literature study when cells are tested on the device for days. As long as an air chamber is designed, there's no additional requirement for the material or working environment. These advantages make the pneumatic actuators be adapted into various kinds of OOCs.

However, as also discussed previously in Section 1.3, pneumatic actuators require

bulky external pressure supplies. This leads to the difficulties of the independent parallel control of multiple devices. In certain OOCs aiming at studying cell behaviour under the impact, the response time of the pneumatic actuator is not fast enough [5]. The design area or the area for cell culture is limited by the space arranged for air chamber. In addition, once the device is fabricated, no spatial control of the direction of the strain is possible since the membrane cannot be tuned by applying prestress or actuated partly.

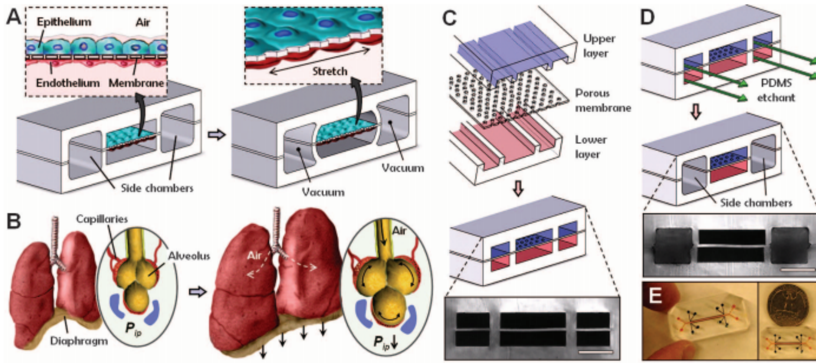

Figure 2.1: 'Lung-on-a-chip'. (A) The OOC device mimics the alveolar-capillary barrier with cells cultured on a porous PDMS membrane. (B) The stretching of the alveolar-capillary barrier in a living lung during inhalation. (C)-(D) Structure of the design. Scale bar, 200 μm. (E) Images of the actual device. [1]

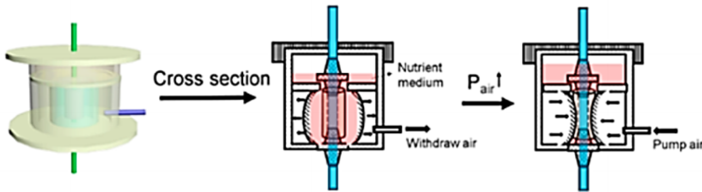

Figure 2.2: Bioreactor for culturing human intestine tissues with pneumatic actuators. The location of the cell culture platform is controlled by pumping or withdrawing air [2].

2.1.2. ELECTRICALLY RESPONSIVE ACTUATORS

DIELECTRIC ELASTOMER ACTUATORS (DEA)

Principle

Dielectric elastomer actuators are in fact capacitors that can expand when voltage is applied (Figure 2.3 [6]). The basic structure of DEAs is a elastomer sandwiched by two compliant electrodes. When voltage is applied, the elastomer will be pressed because of the electrostatic force between two electrodes. Since the elastomer is not compressible, it will contract along the direction of the voltage and expand in the plane perpendicular to that direction. The effective electromechanical pressure p (Maxwell stress) applies on the elastomer is given by equation:

$$p = \varepsilon_0 \varepsilon_r E^2 = \varepsilon_0 \varepsilon_r \left(\frac{V}{d} \right)^2$$

(ϵ_0 is the permittivity of vacuum, ϵ_r is the dielectric constant of the elastomer, E is the applied electric field, d is the initial thickness of the elastomer film [7])

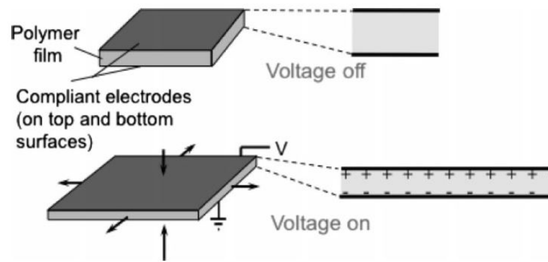

Figure 2.3: The working principle of DEAs. When a voltage is applied, the polymer will expand in area and decrease in height [6].

Three materials are normally adopted in DEAs to create large strain and displacement: silicone elastomer, polyurethanes (PUs) and acrylic elastomers [6]. The specifications of DEAs using different elastomers were summarized by Brochu and Pei [6]. DEAs can be integrated into devices in macro scale, tissue or organ level and single cell level. Three examples regarding these three levels will be introduced in the following.

Applications

A bioreactor using a DEA in macro scale

Figure 2.4 [7] and Figure 2.5 [7] describe a bioreactor designed to mimic the contraction of the intestinal barrier [7]. The device consists of a circular DEA, a rigid frame and a PDMS well to culture cells. The elastomer between the two electrodes is pre-stretched. When voltage is applied, the PDMS well is compressed due to the expansion of the elastomer. This bio-reactor can achieve 10% strain at 4.5kV [7]. Cells cultured 21 days on this bio-reactor were actuated for 4hrs at 0.15Hz to check the strain induced signalling [7].

A DEA to stretch tissue

DEAs can be applied in OOCs to stretch tissue or functional units of an organ. Professor Herbert Shea and his group have been working on developing OOCs using DEAs [5, 8–11]. Figure 2.6 [8] explains one of his works to stretch human tissue in one direction. Before applying the voltage, silicone based elastomer was prestretched both in x and y directions yet non-equibiaxial ($\lambda_x >> \lambda_y$) [8]. Material in x direction became stiffer than y direction, thus the expansion caused by voltage was mainly in y direction. The whole DEA was covered by a biocompatible elastomer. This suggests more freedom to select the dielectric elastomer material in future applications. Lymphatic endothelial cells (LECs) tested on the bioreactor under 10% uniaxial tensile strain at 0.1Hz showed stretch-induced alignment and elongation [8], being a solid proof of DEAs successfully interfacing with living cells.

An array of DEAs to stretch cells

By applying the principle of DEAs, a device to stretch one single cell was designed [9]. 30 μm thick PDMS was selected as the polymer with gold electrodes bonded on the top and the bottom of it. Pyrex substrate with a channel allows uniaxial strain generated since the membrane displacement was constraint by the substrate in the direction perpendicular to the AA line (Figure 2.7 [9]). The final design in Figure 2.8 [9] has an array of 72 microactuators with nine bottom microelectrodes and eight slots on the substrate. Microactuators can be operated in groups at three different frequencies. For one single cell stretcher, 4.7% strain was achieved at a voltage of 2.9kV before buckling [9]. Before the electrical break down of the membrane, a strain of lower than 10% was measured [9].

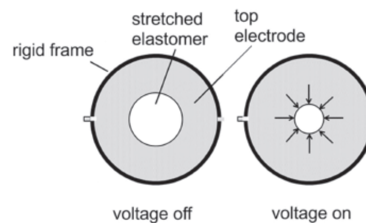

Figure 2.4: Working principle of the bio-reactor to mimic intestinal contraction. The polymer is pushed to the center when the voltage is applied [7].

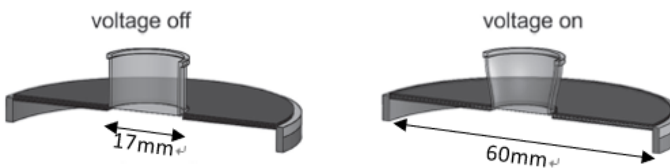

Figure 2.5: The cross section of the bio-reactor to mimic intestinal contraction. PDMS well for cell culturing is compressed by the membrane during the actuated state [7].

2

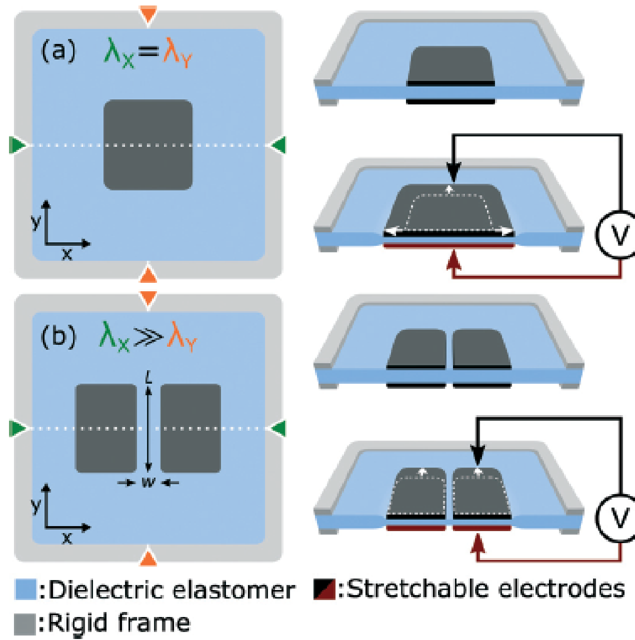

Figure 2.6: Equibiaxial and uniaxial design of the bioreactor. (a) Dielectric elastomer expands equally if prestretching is the same in x and y direction. (b)Elastomer is stiffened in x direction by prestretching. Only the material in the middle of the two electrodes (width=W, length=L) will have cells cultured on top [8].

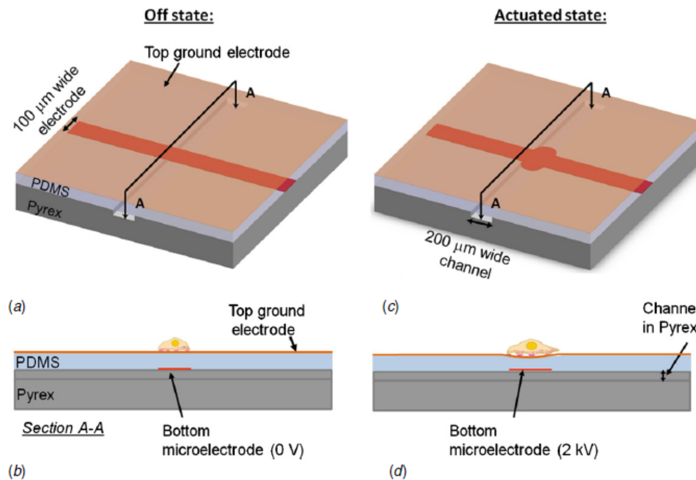

Figure 2.7: Schematics of a single cell stretcher. PDMS is covered on top with a sheet of electrode. The orange stripe indicates the location of the bottom electrode. (b) and (d) are cross sections of (a) and (c). Cells on culture were stretched in AA direction [9].

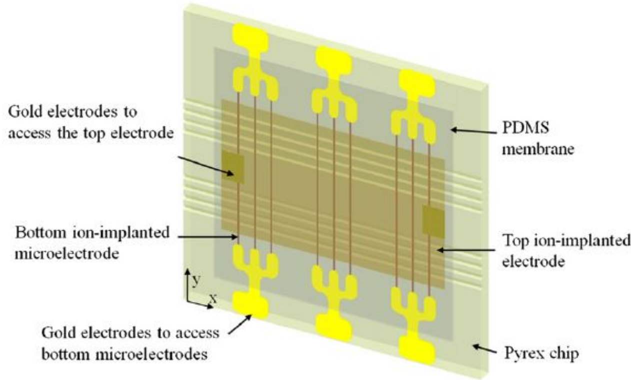

Figure 2.8: Final design of 72 microactuators in three groups [9].

Advantages and limitations

DEAs have the advantages of fast response time, low heat dissipation and silent operation [12]. When integrated into OOCs devices, the direction of the strain can be tuned by controlling prestretching on the membrane. As demonstrated by previous examples, several actuators can be combined into one design and be controlled separately. OOCs using DEAs can achieve a compact design with more design space for microfluidic systems.

Current DEAs are limited by a few problems to be solved before becoming a mature option for OOCs applications. DEAs require high driving electric fields to achieve desired displacement, usually several kV. Because of the applied high voltage, DEAs tend to break down or buckle after several hours of continuous operation. Although lifetime may vary from different designs, DEAs may not be a suitable option for long duration experiments. Besides, the existence of high electric field indicates isolation layers must be considered into OOCs designs to prevent break down inside the device and between the device and measurement tools.

Fabrication of the electrodes for DEA is a future problem for this thesis. In general there are two types of materials that have been used for electrodes, carbon composite or metals, usually gold. Both carbon composite and gold are not cleanroom compatible. Carbon composite electrodes are fabricated by pad-printing, yet it is still unknown whether DEAs with carbon electrodes might break down faster than DEAs with metal electrodes. This concern is proposed because unlike the metal thin film, the particles of carbon composite might diffuse into the polymer, thus leading to an earlier breakdown.

ELECTRO-RESPONSIVE HYDROGELS

Principle

The electro-responsive hydrogel is a kind of synthetic anionic gel that allows positively charged surfactant molecules bind to its surface. Electric field is used to direct the surfactant binding to produce an osmotic pressure difference between the gel interior and the solution outside. This difference leads to the bending of the hydrogel [13] . The driving voltage for electro-responsive hydrogel is low (around several Volt). However,

applying this kind of hydrogel to OOCs remains to be challenging due to its harsh working environment for cells (usually acrylic acid bath).

Application
OOCs directly using electro-responsive hydrogel as actuators were not found during this literature study. However, there is one example using an electro-responsive hydrogel actuator in cell culture media conditions [14]. Figure 2.9 [14] shows an electrically driven hydrogel sorter. A hydrogel strip is in the middle of a microfluidic channel with silver wires positioned at the side. The bending time for the hydrogel from middle to one side is 0.5s at 0.8V [14]. The biocompatibility of the device is tested by sorting mouse embryoid bodies (mEBs). Although the actuator is not at its optimum working environment in the cell culture media, it succeeded in sorting the cells without causing damage [14].

Advantages and limitations
One of the most obvious advantages of the electro-responsive hydrogel is that it can have large deformation at low voltage. This type of actuator has been applied in soft robots design and compliant mechanisms. However, its electromechanical response is relatively slow and dependent on the immersed liquid. These properties indicate that rapid precise control of electro-responsive hydrogel actuators for OOCs is difficult. How to improve its performance in tissue compatible environment remains to be discovered. In addition, this hydrogel may have a leakage problem [15] that could hinder its application in OOCs.

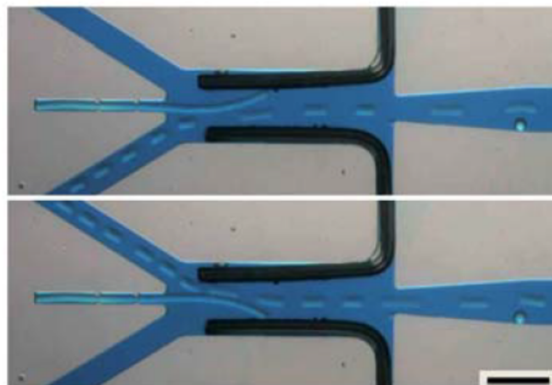

Figure 2.9: A cell sorter using electro-responsive hydrogel. The movement direction of the hydrogel is flipped when the electric potential is reversed. The scale bar indicates 1mm [14].

IONIC POLYMER-METAL COMPOSITES (IPMCS)

Principle
The IPMC is another type of electroactive ionic polymer. Similar to the structure of DEAs, it consists of a polymer sandwiched between two electrodes which allows ion-exchanging [6]. The mechanism of an IPMC actuator is represented schematically in Figure 2.10 [6]. When a bias voltage is applied, mobile ions tend to move to the oppo-

sitely charged electrode, which induce the membrane to swell on one side but contract on the other side, thus eventually leads to the bending of the membrane [16].

Advantages and limitations

IPMCs require low driving voltage (a few volts) for actuation. Studies have demonstrated that IPMCs can be applied to soft actuators or robots, for example, ecological imitation robots from Eamex Corporation in Japan [17]. However, IPMCs have not yet been integrated into OOCs devices or wafer-level microfabrication process. The possibility of applying IPMCs into cell-culture environment in micro-scale devices is still to be discovered.

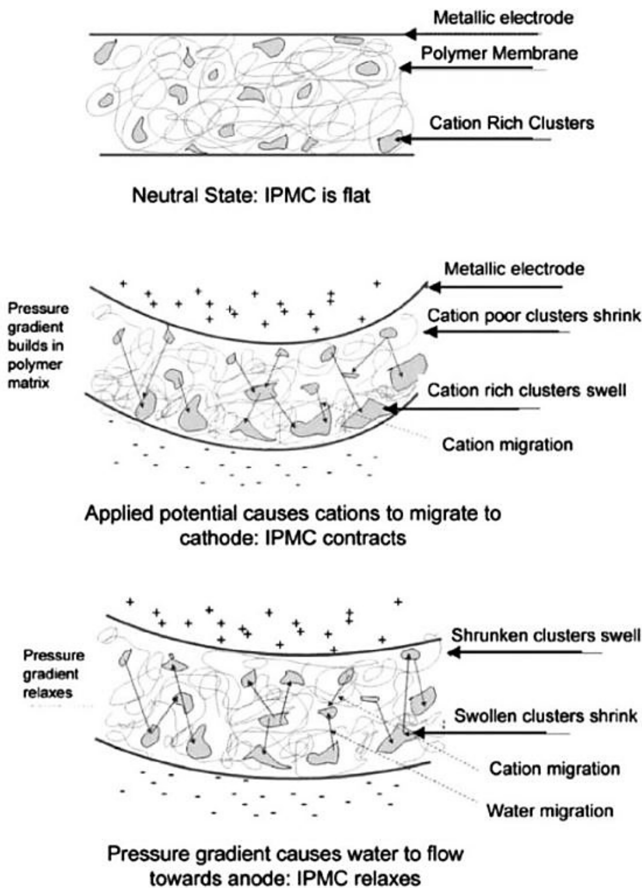

Figure 2.10: A schematic representation of the mechanism of an IPMC actuator [6]

2.1.3. Evaluation and Selection

Before selecting one principle to redesign a polymer-based actuator for Cytostretch, requirements and wishes for the actuator should be specified.

Requirements and wishes
The actuator for Cytostretch should:

- Apply only cyclic stretching to the cells in culture at the frequency of 0.1-5Hz.
- Be bio-compatible.
- Be transparent.
- Can be fabricated using conventional cleanroom compatible microfabrication methods

Apart from the requirements, the actuator for Cytostretch should try to:

- Be as compact as possible.
- Have a long lifetime.
- Allow separate parallel control for multi-well design.
- Be user friendly.

The performances of polymer-based actuators applying different principles as discussed previously and in Appendix A.1 were summarized into a form (Appendix A.2.1). Based on this form and the requirements listed above, a specification form (Appendix A.2.2) was made to help select the principle that could be applied in the design. DEAs were found to meet most of the requirements and revealed possibilities to be applied in Cytostretch. It worth mentioning that even though certain types of actuation principles were promising according to the evaluation forms, they were still not found applied in OOCs designs in this literature study. Given the time length of the master thesis, it is reasonable to select one principle that already has several OOCs applications, not being too ambitious to start an entirely new integration which may require years to complete.

2.2. RESEARCH GOALS AND BOTTLENECKS

The research question of the thesis was the following:

How to design and fabricate a dielectric elastomer actuator for out-of-plane actuation of cell cultures integrated on the Cytostretch platform?

As explained in Section 1.3, DEAs were selected as the basic principle that would be integrated into the actuator design of this thesis. Most of current OOCs use DEAs to induce in-plane strain and displacement. Since the original motion of Cytostretch is out of the membrane plane, a DEAs with similar motion performance can mimic most of its original functionality. Modules, sensors or testing tools designed for Cytostretch can still be applied with minor changes. A DEA with out of plane motion can be adapted into the flow pumping system in future microfluidic system integration, leading to a compact, multifunctional actuation. Therefore, the first research goal is to innovate a DEA that can induce out of plane motion.

In the design of DEA, which will be explained in the design section in Chapter 3, PDMS membrane was sandwiched by the top and bottom electrodes. The fabrication process for putting metal thin film on top of soft substrate like polymers are not yet well defined. Researchers have tried to put gold on top of polymer using low energy implantation [9, 10] or lift off [18]. However, the method for cleanroom compatible metals in general, without using wafer bonding or sacrificial layers to transfer membranes is still a mystery. A wafer-scale conventional cleanroom compatible microfabrication process is expected to be developed to enable batch fabrication of identical devices in shorter time, thus defined as the second research goal.

REFERENCES

[1] D. Huh, B. D. Matthews, A. Mammoto, M. Montoya-Zavala, H. Y. Hsin, and D. E. Ingber, *Reconstituting Organ-Level Lung Functions on a Chip,* Science **328**, 1662 (2010).

[2] W. Zhou, Y. Chen, T. Roh, Y. Lin, S. Ling, S. Zhao, J. D. Lin, N. Khalil, D. M. Cairns, E. Manousiouthakis, M. Tse, and D. L. Kaplan, *Multifunctional bioreactor system for human intestine tissues,* ACS Biomaterials Science & Engineering **4**, 231 (2018).

[3] A. Marsano, C. Conficconi, M. Lemme, P. Occhetta, E. Gaudiello, E. Votta, G. Cerino, A. Redaelli, and M. Rasponi, *Beating heart on a chip: a novel microfluidic platform to generate functional 3d cardiac microtissues,* Lab on a Chip **16**, 599 (2016).

[4] H. J. Kim, D. Huh, G. Hamilton, and D. E. Ingber, *Human gut-on-a-chip inhabited by microbial flora that experiences intestinal peristalsis-like motions and flow,* Lab on a Chip **12**, 2165 (2012).

[5] A. Poulin, M. Imboden, F. Sorba, S. Grazioli, C. Martin-Olmos, S. Rosset, and H. Shea, *An ultra-fast mechanically active cell culture substrate,* Scientific Reports **8**, 9895 (2018).

[6] P. Brochu and Q. Pei, *Advances in dielectric elastomers for actuators and artificial muscles,* Macromolecular Rapid Communications **31**, 10.

[7] D. Cei, J. Costa, G. Gori, G. Frediani, C. Domenici, F. Carpi, and A. Ahluwalia, *A bioreactor with an electro-responsive elastomeric membrane for mimicking intestinal peristalsis,* Bioinspiration & Biomimetics **12**, 016001 (2017).

[8] A. Poulin, C. S. Demir, S. Rosset, T. V. Petrova, and H. Shea, *Dielectric elastomer actuator for mechanical loading of 2d cell cultures,* Lab on a Chip **16**, 3788 (2016).

[9] S. Akbari and H. R. Shea, *Microfabrication and characterization of an array of dielectric elastomer actuators generating uniaxial strain to stretch individual cells,* Journal of Micromechanics and Microengineering **22**, 045020 (2012).

[10] S. Akbari and H. R. Shea, *An array of 100m×100m dielectric elastomer actuators with 80% strain for tissue engineering applications,* Sensors and Actuators A: Physical Selected Papers presented at Eurosensors XXV, **186**, 236 (2012).

[11] A. Poulin, S. Rosset, and H. Shea, *Fabrication and characterization of silicone-based dielectric elastomer actuators for mechanical stimulation of living cells,* in *Electroactive Polymer Actuators and Devices (EAPAD) XX*, Vol. 10594 (International Society for Optics and Photonics, 2018) p. 105940V.

[12] A. Lamberti, M. D. Donato, A. Chiappone, F. Giorgis, and G. Canavese, *Tunable electromechanical actuation in silicone dielectric film,* Smart Materials and Structures **23**, 105001 (2014).

[13] Y. Osada, H. Okuzaki, and H. Hori, *A polymer gel with electrically driven motility,* Nature **355**, 242 (1992).

[14] G. H. Kwon, Y. Y. Choi, J. Y. Park, D. H. Woo, K. B. Lee, J. H. Kim, and S.-H. Lee, *Electrically-driven hydrogel actuators in microfluidic channels: fabrication, characterization, and biological application,* Lab on a Chip **10**, 1604 (2010).

[15] L. Hines, K. Petersen, G. Z. Lum, and M. Sitti, *Soft Actuators for Small-Scale Robotics,* Advanced Materials **29**, 1603483 (2017).

[16] M. Shahinpoor, Y. Bar-Cohen, J. O. Simpson, and J. Smith, *Ionic polymer-metal composites (IPMCs) as biomimetic sensors, actuators and artificial muscles - a review,* Smart Materials and Structures **7**, R15 (1998).

[17] *Eamex co.japan,* .

[18] L. Guo, G. S. Guvanasen, X. Liu, C. Tuthill, T. R. Nichols, and S. P. DeWeerth, *A PDMS-Based Integrated Stretchable Microelectrode Array (isMEA) for Neural and Muscular Surface Interfacing,* IEEE Transactions on Biomedical Circuits and Systems **7**, 1 (2013).

3

Design and Fabrication of Dielectric Elastomer Actuators for Organ-on-Chip Platforms

3.1. Introduction

Polymer-based actuators, having the advantages of being compliant, lightweight and biocompatible, are attractive options for OOC platforms. The dielectric elastomer actuator is a kind of polymer-based actuators that can induce large displacement under high voltage [1]. DEAs can be applied to design macro scale bioreactor [2], a uniaxial tissue stretcher [3] or arrays for single cell stretching [4]. Most DEA devices have in-plane stretching. A DEA for out-of-plane actuation is expected to reveal more application possibilities. For this thesis in particular, a DEA with out-of-plane motion is developed for a previous OOC platform, Cytostretch [5].

Fabricating DEAs in microscale is challenging due to the difficulty of depositing and patterning electrodes on top of a membrane, being a soft substrate different from the conventional one. Researchers have successfully put gold electrodes on top of polymer using low energy implantation [4, 6] or lift off [7]. However, there are few experience for depositing and patterning electrodes on soft substrate using conventional cleanroom compatible process.

In this thesis, a DEA for out-of-plane actuation is designed for Cytostretch. Its functionality is proved by using numerical analysis. Difficulties of complex microscale multilayer material modelling and converging the buckling problem is discussed. Process flow for fabricating TiN electrodes on top of PDMS is developed and tested using conventional cleanroom microfabriation methods.

3.2. Design

In this section, the design and structure of the DEA for Cytostretch is described. First the basic idea and structure of the actuator is introduced, followed by the final design and its 3D model. The objective of the design, as also mentioned in Chapter 1, is a DEA that can induce out of plane motion and cyclic stretch the tissue in culture.

The basic idea of the DEA actuator is a suspended PDMS membrane sandwiched by electrodes from two sides as shown in Figure 3.1. When a potential difference is applied between top and bottom electrodes, the membrane tends to decrease in height and expand in x and y directions. However, the expansion in area is partially constrained by bonding the membrane to the substrate. As PDMS is not compressible, more material will be pushed to the free-standing area and lead to buckling of the membrane (Figure 3.2).

Cells or tissue will be cultured in the center area which does not covered by the electrodes, or on possible topology structure on the membrane. This is due to the consideration that the optical transparency in the middle area is helpful to allow alignment and measurement under standard microscope. The high voltage will be applied to the bottom electrodes underneath the PDMS membrane. Top electrodes, which has the possibility to be exposed to the cell culture medium is grounded. This isolates the cells from getting contact with high voltage directly.

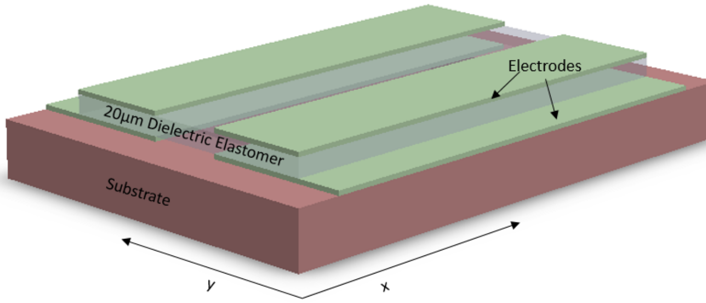

Figure 3.1: Conceptual design of the DEA: A suspended dielectric elastomer membrane with top and bottom electrodes from two sides. A rectangular opening is in the center of the substrate from the backside to make the membrane suspended. The thicknesses of each layer are not drawn on the exact scale.

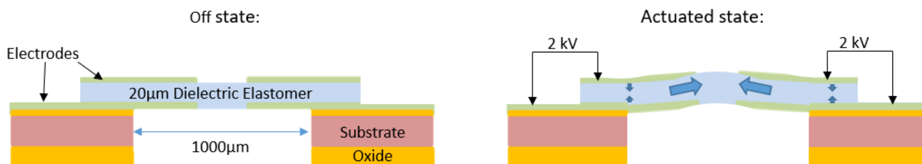

Figure 3.2: Cross section of the DEA design in off state and actuated state. The blue arrows marked on the actuated state indicates the movement direction of the dielectric elastomer. Thicknesses of each layer are not drawn on the exact scale.

A simple 2D estimation is made to calculate the possible displacement of the center point of the membrane. The thickness of the PDMS and the difference in thickness before and after the applied potential field is neglected. The original length is assumed to be $1000\mu m$ and the expansion is uniform. As shown in figure 3.3, if the PDMS expands 10% in length and the arc formed after the actuation is perfect, the displacement of the center is roughly $190\mu m$. This calculation is very rough and only for a referential estimation of the displacement.

Although the initial design concept seems simple, several modifications are necessary before it can be actually fabricated. The bottom electrodes should be properly insulated since it will be connected to high voltage supply. Insulation layers help to eliminate electric fringe field through the air. For the top electrodes, a buffering layer between the metal and PDMS should be designed. The reason will be explained in Section 3.3. Lastly, in order to make the actuator compatible to future tool holders or Printed Circuit Board (PCB), aluminium contact pads for wire bonding were added to the design. The final design, as shown in Figure 3.4 , is a complex stack which makes the fabrication very challenging.

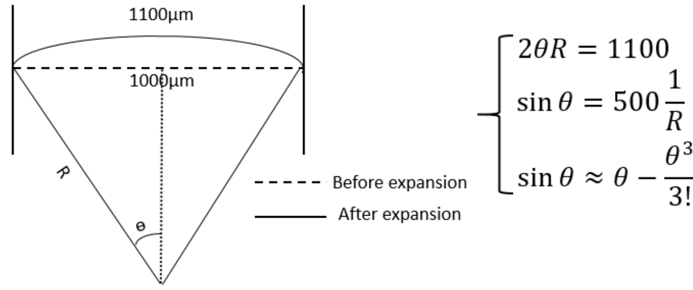

Figure 3.3: A simple estimation of the displacement of the membrane center after actuation. Equations are based on the figure on the left. The original location of the membrane is represented by the dot line and membrane after actuation is the solid curve. A group of equations on the right can be deducted from the left figure to calculate the value of θ. The height difference between the plat membrane and actuated membrane can be estimated based on θ.

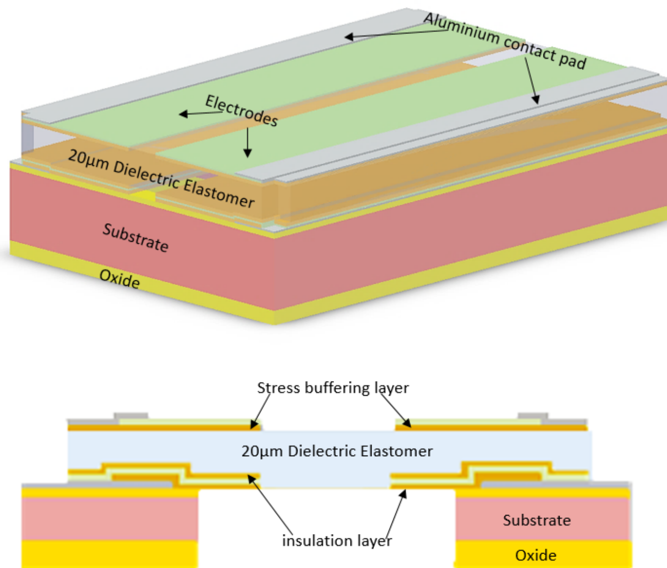

Figure 3.4: Final design of the DEA with electrodes insulation, stress buffering and contact pads. Top: 3D model of the DEA. Bottom: cross section of the DEA. Thicknesses of each layer are not drawn on the exact scale.

3.3. MATERIAL SELECTION

PDMS MEMBRANE

In order to achieve desired mechanical stretching and reduce the corresponding voltage, polymers with relatively high dielectric constant should be considered as the material for the membrane (refer to Section 1.3.2). A table summarizing properties of different

dielectric materials was provided by scholars [1]. Compared to acrylic elastomers (commercially available from 3M), the dielectric factor of PDMS (2.8) is relatively low. However, as a silicone elastomer, PDMS has the advantage of low viscoelastic behavior which can guarantee the actuation frequency and the repetitive strain [1].

Another important reason to select PDMS as the membrane material is the availability of the material and fabrication processes. Compared to the other dielectric materials, PDMS has the advantages that mature guidelines for depositing and patterning PDMS in conventional cleanroom compatible microfabrication processes have been established in the ECTM group. Indeed there is a possibility that certain other polymers may have better performance than PDMS for the DEA design. This can be further explored in future to optimize the DEA devices.

Since the performance of the DEA design for Cytostretch has to be estimated numerically in COMSOL Multiphysics, a series of tensile tests were carried to characterize the mechanical properties of PDMS for simulations. As shown in figure 3.5, a PDMS sample was clamped in the Dynamic Mechanical Analyzer(DMA) (TA instruments, Q800). The sample was pulled until it broke and Young's modulus of the sample can be calculated via equation 3.1. The results of measured Young's modulus of PDMS is listed in table 3.1.

$$E = \frac{\frac{F}{A}}{\frac{dl}{L}} \tag{3.1}$$

(F is applied force, A is force applied area, dl is change of the length, L is the length of the sample)

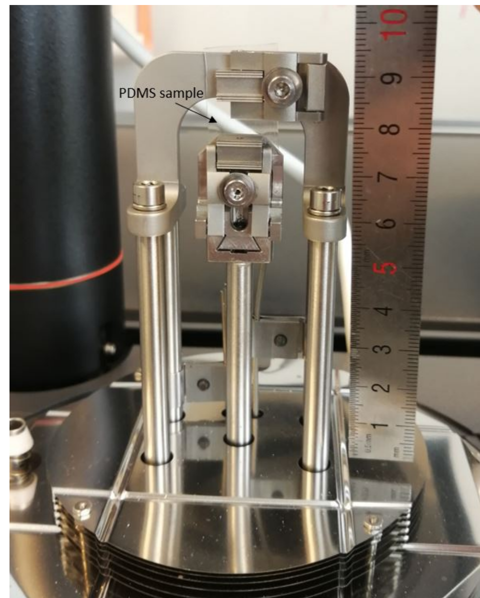

Figure 3.5: A PDMS sample clamped on the Dynamic Mechanical Analyzer (DMA) (TA instruments, Q800) for tensile testing

Group No.	PDMS Mixing ratio (Base: Curing agent)	Young's modulus (MPa)
1	5:1	0.510
2	10:1	0.297
3	10:1	0.865
4	10:1	0.867

Table 3.1: Young's modulus of PDMS with different mixing ratio. The result of each group is the average of three measurements

It can be observed from table 3.1 that Young's modulus of first two groups are much smaller than literature (around 1MPa for PDMS with mixing ratio 10:1 [7]). There are two possible reasons might explain the smaller values. First, the PDMS samples for group 1 and 2 were cured at room temperature for 24h. Although the time should be sufficient to fully cure the PDMS, there might be a chance that the samples tested in group 1 and 2 were not fully cured. Second, when clamping the PDMS samples on the tensile tester, it is possible that not sufficient force was applied so the sample slid while being stretched.

Testing group 3 and 4 were therefore designed to measure the Young's modulus of PDMS again. This time the PDMS was cured for 1h at 90 degrees Celsius in the oven. It should be noted that the petri dish for preparing the sample was not melted but got soft under this curing condition (Figure 3.6). Results measured from these two groups are closer to the value found in literature. However, there was still a chance that samples slid during testings. This error cannot be fully eliminated since PDMS samples would be crushed and torn directly if too much clamping force was applied. PDMS can only be clamped 'relatively tight'. The average of the Young's modulus measured in group 3 and 4 (0.866 MPa) was used later in the numerical simulations.

Figure 3.6: A twisted petri dish. The petri dish became soft in the oven for 1h at 90 degrees Celsius. Yet it was not sticky or melted

TITANIUM NITRIDE (TIN) ELECTRODES

The microelectrodes for the original Cytostretch was made of TiN. The new DEA design continues to use TiN as electrodes. TiN has several advantages to be applied in bioelectrode applications [8], mostly from fabrication perspectives. First it can be deposited at room temperature, which is critical to the design as the polymer cannot undertake high

temperature processes. Second it can be easily patterned with standard lithography and plasma etching. It does not cause contamination problem inside the cleanroom. In addition, the material is chemical stable and demonstrates good biocompatibility [8].

TiN may have the problem of very high impedance. There is research work inside ECTM group to find low impedance alternatives such as carbon nanotube (CNT) and polymers such as PSS-PDOT. However, for the specific design of DEA, the high impedance does not influence much on the DEA performance. In theory, a DEA requires little to no current to operate once it is stabilized. Although the functionality of previous DEA devices with gold or carbon composite as electrodes has been proved (refer to chapter 1.3.2), one of the research goals as mentioned before is to deposit and pattern electrodes on soft substrate (PDMS) using conventional cleanroom-compatible processes.

POLYIMIDE (PI) INSULATION AND STRESS BUFFERING LAYERS

As mentioned in previous design section, the bottom TiN electrodes need to be properly insulated. During the fabrication process of Cytostretch, parylene was first chosen as the insulation material. However, the fabrication process of parylene was found complicated and making the tool cleanroom incompatible [9]. In addition, etching parylene results in vertical profiles that can cause step coverage problems when depositing metals on top of it [10]. Polyimide, being commonly used in microelectronics, was selected later for the insulation layer material. Showing good chemical resistance [11] and good mechanical properties [12], PI can be deposited by simple spin coating. PI LTC9305 from FUJIFILM was applied in the fabrication process for DEA. It is photosensitive and can form a thin layer around 1 μm.

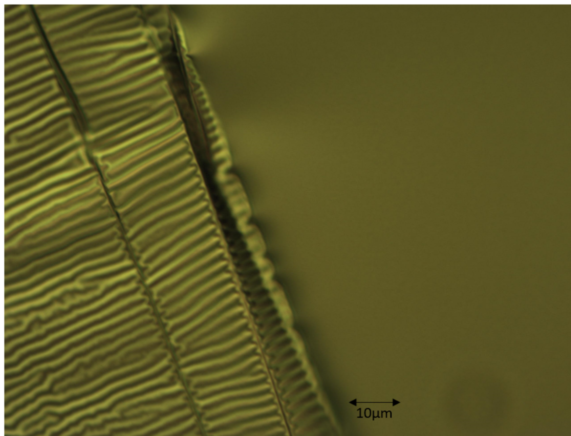

Figure 3.7: Contrast of surface topology of TiN landing on PDMS (Young's modulus around 1 Mpa [7]) directly (left) and with PI (Young's modulus around 1Gpa [7]) buffering layer (right)

For the electrodes on top of the PDMS, directly depositing TiN was tried in the beginning. However, the depositing TiN on PDMS process generated much stress that caused many wrinkles on the surface (left half of Figure 3.7). Wrinkles of this size destroyed the TiN thin film and led to delamination. The rough surface may lead to severe adhesion

problems for the following steps. Therefore, a stress buffering layer is needed to fabricate top electrodes. PI (Young's modulus around 1Gpa [7]) was tried as the buffering layer and successfully reduced the generation of wrinkles (right half of Figure 3.7).

3.4. FINITE ELEMENT ANALYSIS

Numerical analysis of the DEA actuator is carried out in COMOSL Multiphysics to estimate the deflection of the devices. A $2000\mu m x 3000\mu m$ platform was meshed with a $20\mu m x 1000\mu m x 2000\mu m$ suspended membrane in the center. The geometry dimensions are marked in Figure 3.8 and material properties are listed in Table 3.2. For the membrane area that should be sandwiched between the electrodes and PI insulation/buffer layers, the difference of Young's modulus was considered. If the stack of PDMS, TiN and PI were piled and modeled directly, there was a meshing problem caused since the thickness of PI ($350nm$) and especially TiN ($100nm$) were very small compared to PDMS ($20\mu m$). This meshing problem led to long time calculation and could not converge.

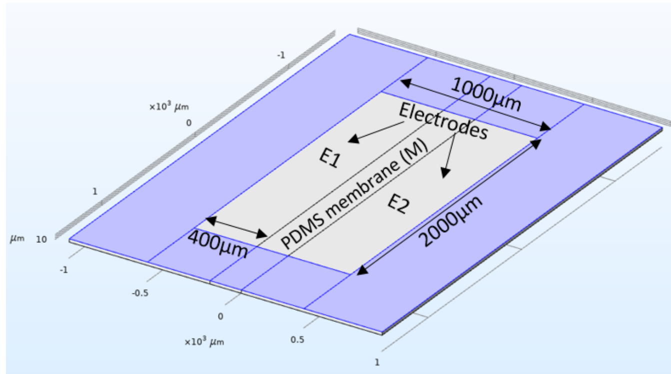

Figure 3.8: Geometry of the PDMS membrane applied in simulation. Violet area has a fixed boundary constraint at the backside representing the membrane was bonded to the substrate. Area E1 and E2 are the PDMS area sandwiched by TiN electrodes which were considered as a lumped material with effective Young's modulus. Area M is the free-standing PDMS cell culture area. Voltage potential was applied between the top and bottom electrodes

Area	Young's modulus	Poisson's ratio	relative permittivity
pure PDMS membrane M	0.866 MPa	0.49	2.75
lumped PDMS (E1 & E2)	50.7 MPa	0.49	2.75
PDMS with Gold electrodes[4]	2.5 MPa	0.49	2.75

Table 3.2: Material properties used in the FEM simulation

A lumped method was adopted to solve this meshing problem. The stack was considered as a whole block and a combined Young's modulus was applied. I were not able to actually measure the Young's modulus of PDMS with PI layers and deposited TiN electrodes. Therefore, the effective Young's modulus was calculated using the mathematical model in Appendix A.3 and result listed in Table 3.2 line 2. One assumption in this

lumped model is that the adhesion between different layers is perfect and no relative slide would occur during the whole actuation process.

However, the calculated effective Young's modulus of the lumped model may not represent the real situation. The actual value of the Young's modulus can be influenced by the adhesion between each layer and the topology of TiN. Similar to the previously discussed issue of PI stress buffering layer, TiN landing on PI may still have small wrinkles. The wrinkles can work like small 'springs' in the complex stacks during tensile testing, thus influence the final value of the Young's Modulus. There is a measured Young's modulus of 30μm thick PDMS with double side ion-implanted gold electrodes in literature [4] as listed in table 3.2 line 3. This value was also applied in COMSOL and will be discussed in comparison with the effective Young's modulus of lumped PDMS.

After the pre-force, a voltage was then applied between the top and bottom electrodes. The fixed area (violet area) as shown in figure 3.8 represents the membrane that would be bonded to the substrate (in x and y direction). A small pre-force was applied to the membrane to disturb the symmetry of this buckling problem so that it can be converged in COMSOL. After a coupled field analysis, the computed displacement was plotted in Figure 3.9 and Figure 3.10. It can be observed that the center of the membrane achieved a displacement of 7.35μm under 3000V using the calculated effective Young's modulus (50.7MPa) and 44.7μm under 2167V using the measured Young's modulus with gold electrodes found in literature (2.5MPa). Figure 3.11 displays the displacement of the membrane center versus different voltage applied between the top and bottom electrodes.

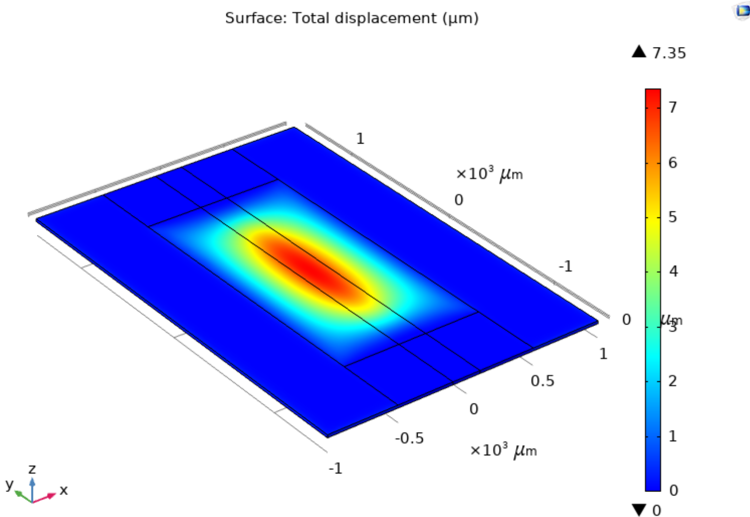

Figure 3.9: Profile of the displacement of the membrane when a voltage of 3000 V was applied to the electrodes. In this model, the effective Young's modulus of the lumped PDMS-electrodes area (50.7 MPa) was applied

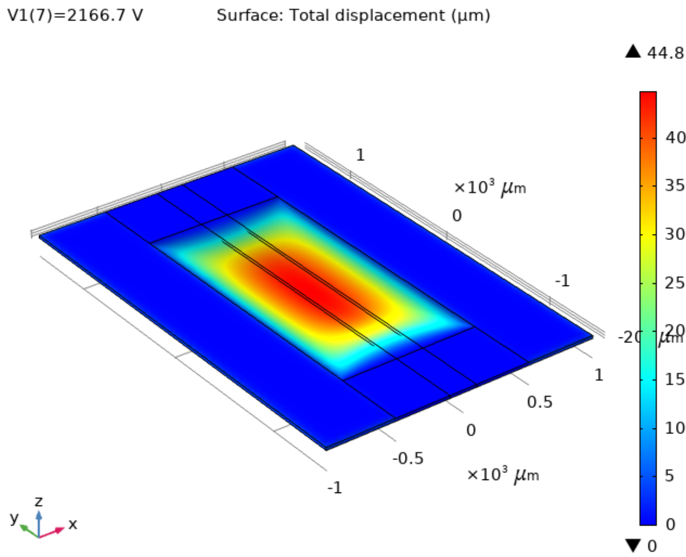

Figure 3.10: Profile of the displacement of the membrane when a voltage of 2166.7 V was applied to the electrodes. In this model, the measured Young's modulus of a PDMS membrane with double-side gold electrodes (2.5 MPa [4]) was applied.

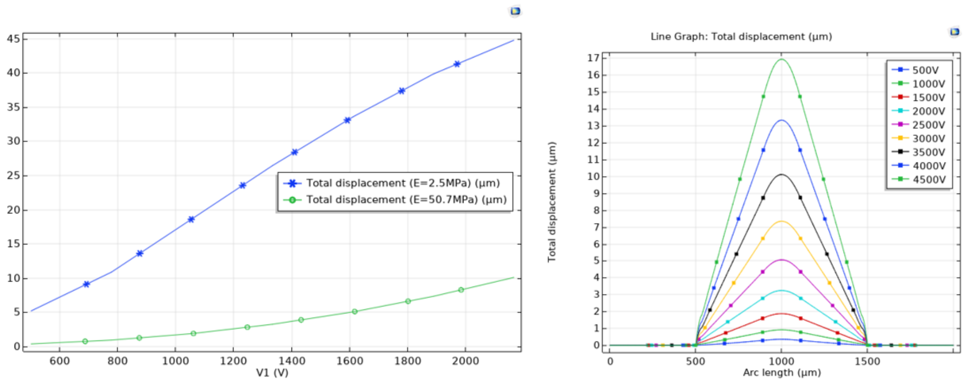

Figure 3.11: Left: Displacement of the membrane center verses applied voltage of the DEA. Two different values of Young's modulus were applied in the area of PDMS sandwiched between electrodes. Right: Cross-section displacement profile of a DEA membrane under different voltage. Effective Young's modulus (E=50.7 MPa) calculated using the lumped method was applied. Arc length indicates the distance from one edge of the membrane which was set to be the starting point of the line plot.From 500μm to 1500μm are the area of the suspended membrane (refer to Figure3.8).

The reason to apply two Young's modulus obtained from different sources for the PDMS area with top and bottom electrodes (Area E1 and E2 in Figure 3.8) is twofold. First, since no tools or process were directly available to measure the Young's modulus of a stack of multiple materials on a wafer during the time given for thesis, the actual value of the Young's modulus can only be estimated. Comparing the simulations results using different Young's modulus for Area E1 and E2 can help better understand the mechanism of DEA. Second, after the fabrication and characterization process of DEA full devices, the performance of the DEA can be used to trace back the actual Young's modulus of Area E1 and E2, based on current simulation results using different values of Young's modulus.

Another issue that should be discussed is the convergence problem in buckling problem modelling in COMSOL. It has been noticed that the model can only converge on certain discontinuous range of applied voltage. The actuated shape of the membrane also behaved with certain 'mode shapes'. One assumption to explain the discontinuous convergence problem is that the stability of the membrane will reach a 'mode switching point' while increasing the applied voltage between the electrodes. Simulation cannot converge until a new stability can be achieved under higher voltage after the switching point.

3.5. FABRICATION

One of the research goals of this thesis is to deposit and pattern metals on top of soft substrate using conventional cleanroom compatible microfabrication. This issue was identified and addressed gradually in the fabrication processes of a complete DEA as described in previous chapters. In the beginning, the whole fabrication flowchart for a DEA was designed with detailed recipes, which can be found in Appendix A.4.

The main fabrication steps can be summarized into a schematic diagram as Figure 3.12. First, bask side silicon dioxide (SiO_2) was patterned on a double side polished wafer to define the suspended membrane area, functioning as a hard mask for releasing the membrane in the end. Then, the aluminium bottom contact pad was deposited and patterned. Later the bottom TiN electrodes were placed with a PI-TiN-PI insulation structure. $20\mu m$ PDMS was spin coated on top of the electrodes. Finally, top TiN electrodes were patterned with a PI buffering layer. After patterning the PDMS and releasing the membrane, the DEA full devices will be fabricated.

Fabrication experience is already available for the structures underneath PDMS in our research group, referring to the bottom aluminium contact pad and PI-TiN-PI stack. Although the patterns were different, a similar sequence of depositing and patterning material has already been applied in the original Cytostretch fabrication. However, little information was found to fabricate the structure on top of PDMS. Therefore, the fabrication process was focused on how to deposit and pattern metals on top of soft substrate (Figure 3.13), addressed as one of the research goals. Several issues were identified and solved during this process, which will be explained in the later sections.

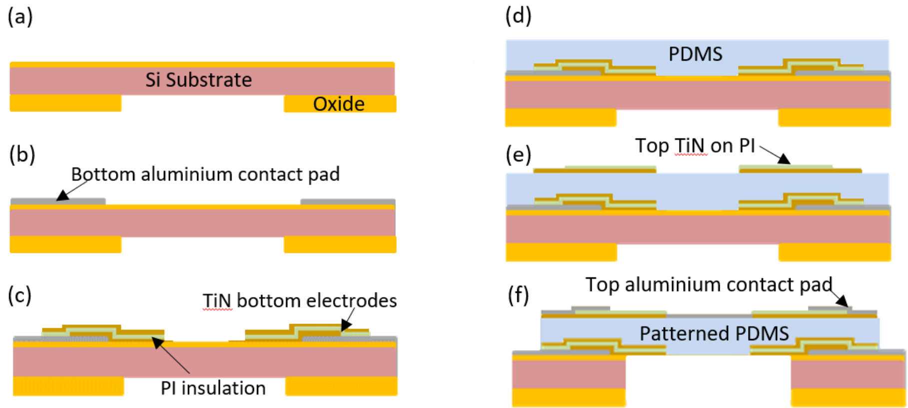

Figure 3.12: Fabrication flow of the designed DEA: (a) SiO_2 deposition and backside patterning. (b)Bottom aluminium contact pad deposition and patterning using conventional lithography. (c) TiN bottom electrodes deposition and patterning encapsulated by PI insulation layers. (d)PDMS spin coating (e) Top TiN electrodes deposition with PI stress buffering layer (e) Top aluminium contact pad and PDMS etching

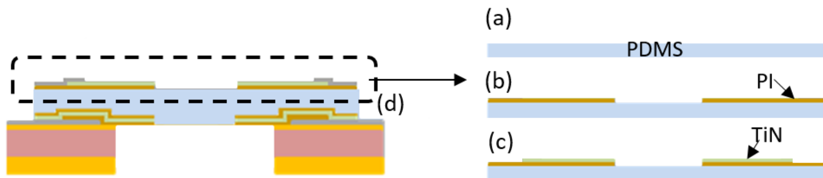

Figure 3.13: Fabrication flow of the top TiN electrodes for DEA: (a) Spin coated PDMS soft substrate (b) PI deposition and patterning (c) TiN deposition and patterning (d) PDMS etching

3.6. RESULTS

3.6.1. PDMS-PI ADHESION

The adhesion issue between PDMS and PI can be observed in Figure 3.14 (a). The thin film of PI immediately broke after the spin coating on PDMS. Certain treatment was tested to change the hydrophobic natural of PDMS thus improve the adhesion. Previously in the work for Cytostretch, argon plasma was applied to modify the surface of PI before putting PDMS [9]. However, given the equipment availability of the cleanroom, only low energy oxygen plasma was possible to treat the surface during the fabrication process of this thesis. After treating the PDMS surface 30s using 75W oxygen plasma, the adhesion between PDMS and PI was strongly improved as a smooth uniform PI thin film was successfully deposited.

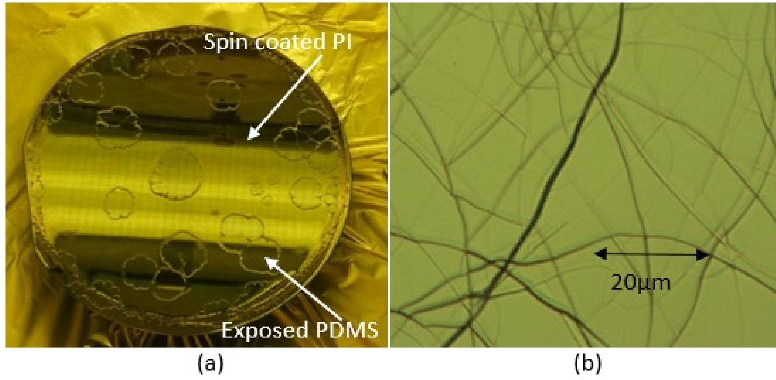

Figure 3.14: (a) 1 minute after spin coating PI on PDMS on a 4 inch wafer. Thin film of PI broke and PDMS underneath was exposed. (b)Cracks on PDMS after oxygen plasma treatment at 1000W with endpoint detection

The influence of low energy oxygen plasma treatment on PDMS to promote PI-PDMS adhesion can be explained with three mechanisms. First, the plasma can bombard the polymer surface and lead to a rougher surface, initiating a PDMS-PI interlocking. Second, the treatment increases the amount of -OH group, changing the surface from hydrophobic to hydrophobic. Third influence, however, being negative to the process, might lead to the cracking of PDMS (Figure 3.14(b)). In the beginning, the surface of PDMS will be oxidised and form a silica-like crust after exposure to oxygen plasma [13]. Further treatment will cause the 'crust' being mechanically stressed and initiate a spontaneous cracking on the surface. The correct dose of the oxygen plasma to treat the PDMS surface was tried for several times before the recipe of 30s at 75w was finalized.

3.6.2. PI DEPOSITING AND CURING

After the low energy oxygen plasma surface treatment process, the PI should be immediately deposited, patterned and cured as soon as possible (less than half day). This is because the improved surface adhesion is temporary and PDMS surface will return to its natural hydrophobicity. Figure 3.15(a) presents the ruptured thin film of PI on top of PDMS cured after waiting overnight (around 10 hrs). As for depositing PI, the thickness is suggested to be roughly 350nm. Although ideally the thickness of PI should try to be as thin as possible, the surface of PI thin film will become nonuniform when it is too thin.

To pattern the PI thin film, it should be noted that the time for soft bake and post exposure bake should be extended. Figure 3.15(b) is a picture of PI detached from the PDMS layer during developing due to insufficient soft baking and post exposure bake. Since PI was baked on the hot plate with thick (20μm) PDMS layer underneath, the original baking time was not sufficient. This problem was first observed and solved by increasing baking time with PI durimide 7020 but the solution applied to PI LTC9305 as well for fabricating the DEA full device.

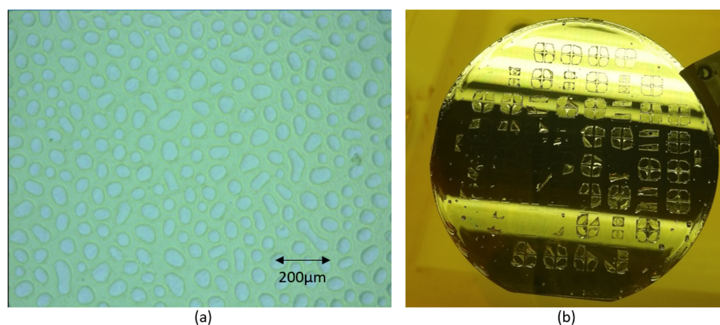

Figure 3.15: (a)Ruptured PI surface on PDMS after around 10 hrs without curing. (b) Delamination of PI during developing process on a 4 inch wafer

Last issue caused by PI is the curing process. Standard curing temperature and time for Polyimide is 60 minutes at 350 degrees. However, this temperature cannot be reached when the structure has PDMS. A special curing recipe (Appendix A.6) was developed to cure the PI at a lower temperature using a longer time. After cured with the special recipe, the wafer with PI-PDMS structure was soaked into Acetone and HTR-D2 developer separately for 10 minutes to check if the PI was fully cured. There was no delamination observed after the tests. The curing process was checked again with the Leak-up-Rate (LUR) test in Trikon SigmaEVG 204. The PI was considered to be fully cured as it passed the LUR test.

3.6.3. TiN depositing and patterning

100μm TiN was deposited at room temperature and landed on PI for the top electrodes of DEA. Figure 3.16 (a) and (b) are pictures of TiN landing on PDMS with and without PI buffering layer. The clear and blurry reflections of my phone indicate the different roughness of the surface (Also refer to Figure 3.7). TiN was then etched in Trikon Omega 201 plasma etcher. The etching time should be strictly calculated to avoid over etching since endpoint detection is not directly available for etching TiN.

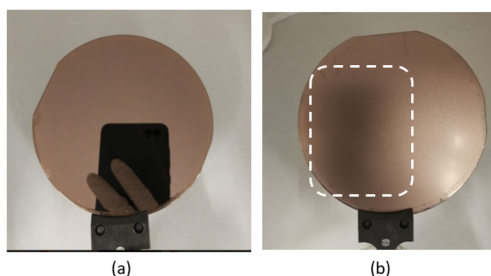

Figure 3.16: (a) TiN deposited on PI-PDMS stack on a 4 inch wafer. The reflective surface indicates a smooth surface (b) TiN deposited directly on PDMS on a 4 inch wafer. A blurry reflection of my phone can be seen in the white frame. This indicates a relatively rough surface

Removing photoresist (PR) after etching TiN was tricky. The PR was bombarded during the etching process therefore, formed a hard surface very difficult to remove. There were two conventional methods to remove PR, oxygen plasma or acetone. Figure 3.17(b) is a picture of TiN top electrodes using Tepla Plasma 300 at 1000W with endpoint detection to remove PR. It can be observed that the PI buffering layer was removed together with PR and the TiN surface became full of wrinkles. If the plasma dose was decreased to 1 minute at 600W, the PR on the other hand, cannot be removed. The colorful surface of the wafer in Figure 3.17 (a) indicates the nonuniform residual layer of PR. It was measured that the thickness of PR decreased around 100nm after the plasma, yet the original thickness was 1.4μm. Acetone was tried to remove PR as well. Figure 3.17 (c) shows the PR chips on top of TiN after soaking the wafer in acetone for 5 minutes with gentle stirring. The PR was cracked and some of the PR was removed, yet PR residues were still found. The solution is to combine the two methods: First treat the PR with plasma at 600W for 1 minute. Then use the acetone bath at room temperature for 5 minutes. The 1 minute 600W oxygen plasma cleaning was applied again in the end. A PR-free wafer with patterned TiN electrodes on top of PDMS with PI buffering layer was shown in Figure 3.18.

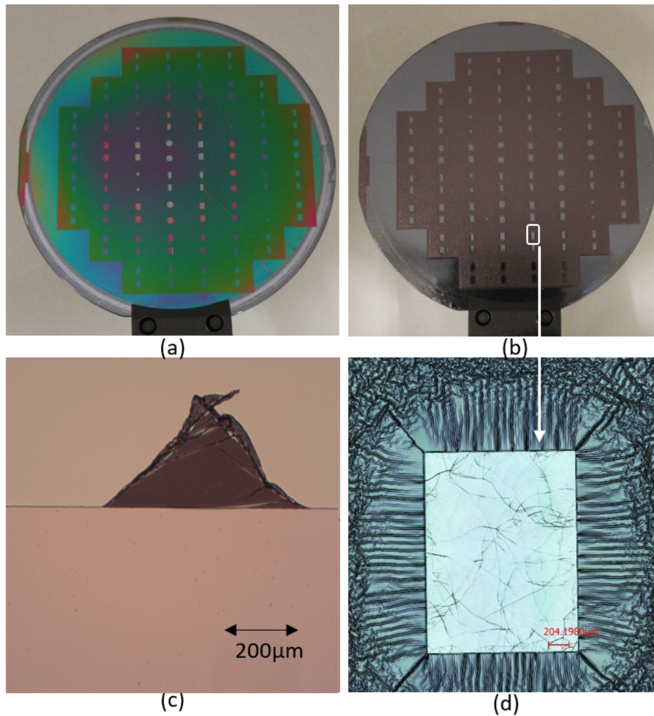

Figure 3.17: (a) PR layer on TiN after oxygen plasma cleaning 1 minute at 600W (b) Wrinkled TiN after oxygen plasma cleaning at 1000W with endpoint detection. (c) PR residue after cleaning the PR with acetone bath (d) Close up of one pattern to show the cracked polymer (light blue area) and wrinkled TiN surface

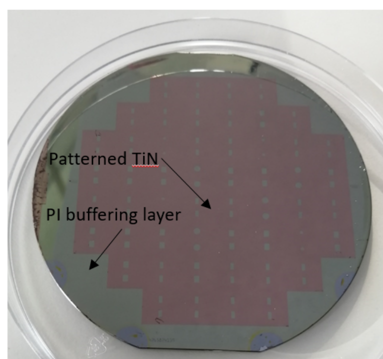

Figure 3.18: Patterned TiN on top of PDMS with PI buffering layer (TIN-PDMS-PI) on a 4 inch wafer

3.6.4. PDMS ETCHING

Etching PDMS membrane after patterning TiN electrodes was tested at last. An aluminium hard mask was patterned using conventional lithography as common PR cannot stand the long etching duration. The recipe for etching PDMS also removes SiO_2 and the Si substrate, therefore it was difficult to define the exact etching time since there was no relative zero point to measure the step height. Overetching PDMS was almost inevitable.

Before etching, lines of cracks was observed on certain area of the PDMS which was not covered by the aluminium hard mask. One possible explanation of the cracks is that during the patterning of aluminium hard mask, the plasma induced silica-like crust on PDMS surface (similar to oxygen plasma surface treatment) and later cracked due to the stress. After etching, the aluminium hard mask was removed by wet etching. Fortunately, no cracks was observed on the patterned PDMS. Figure 3.19 are photos of PDMS before and after etching.

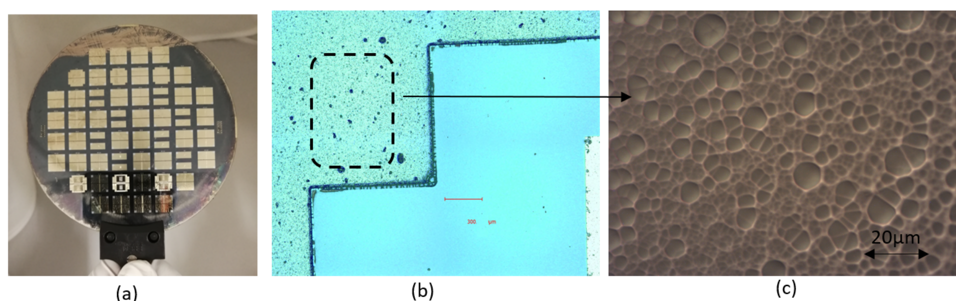

Figure 3.19: (a) Aluminium hard mask for PDMS etching on a 4 inch wafer (b) Over-etched PDMS (smooth blue area) (c) The rough Si surface after PDMS etching

3.7. DISCUSSION

The fabrication process of the full DEA devices can be completed by releasing the membrane from the backside after PDMS etching, However, the process wafer was accidentally broken during the manual drying process. Unfortunately, certain tools for process-

ing were down and developer for PI was running out. There was not enough time to fabricate a new batch of DEA full devices before the submitting this thesis. However, as discussed in the result section, all critical steps in the fabrication flow have already been developed and tested. It can be predicted that DEA full devices can be fabricated smoothly given the availability of tools and chemicals.

Figure 3.20 (a) (b) (c) (d) are pictures of successfully deposited TiN electrodes (TiN-PI-PDMS stack) with etching holes of different shapes and dimensions under the microscope. The surface of TiN was flat in general yet wrinkles were found at the corners of certain etching holes. The dimensions of the wrinkles were measured and calculated. Together with different dimensions of the etching patterns, the measured results of wrinkles are listed in table 3.3. The wrinkle size was compared with Figure 3.20 (e) which shows the same patterned TiN directly on PI without PDMS (TiN-PI stack). Except the PDMS layer, all the other steps to fabricate these two wafers were the same. It can be suggested that the thermal expansion of PDMS during etching steps was the cause of the wrinkles.

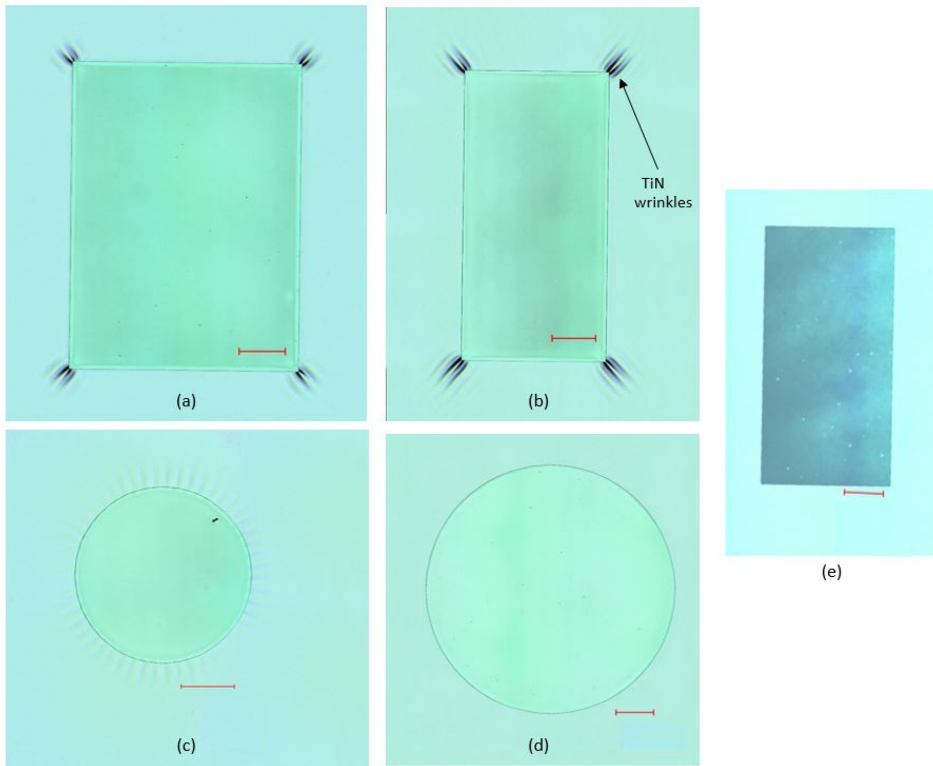

Figure 3.20: (a)-(d)TiN deposited on PDMS with PI as stress buffering layer (TiN on PI-PDMS stack). Different geometry of holes were etched to check the influence of the etching. Red bar in all pictures represents $300\mu m$ (a) rectangular $1.5mmx2mm$ etching hole (b)rectangular $1mmx2mm$ etching hole (c) circle diameter=$1mm$ etching hole (d) circle diameter=$2mm$ etching hole (e) TiN deposited on only PI layer without PDMS. Rectangular $1.5mmx2mm$ etching hole

From the pictures and the measurement results, two assumptions were proposed. First, the appearance of the wrinkles are related to the angle of the corner. One explanation of the existence of wrinkles in 3.20 (c) is that during mask design, the circle pattern was not a perfect circle but approximated with polygons, therefore, there were still very flat 'corners' even we cannot see directly. Comparing the etching holes of rectangular and circles, it can be proposed that the height difference of the wrinkles decrease with the angles of the corner being more flat. Second, the size of the etching holes can influence the height difference of the wrinkles. Comparing the two samples inside rectangular group and circle group respectively, the height difference decrease when the sizes of the holes are bigger. More samples are needed for future to testify the two assumptions and eventually conclude a quantitative theory.

shape	dimension (mm)	wrinkles	maximum height difference (μm)
rectangular	1.5x2	at corners	0.39
rectangular	1x2	at corners	0.53
circle	D=1	around edges	0.12
circle	D=2	no	-

Table 3.3: Measurement results of wrinkles of etch holes with different shape or geometry

3.8. Conclusion

This thesis has presented the design and numerical analysis of a DEA for OOC platforms, fabrication of TiN electrodes on top of soft substrate and basic measurements of the fabrication results. The DEA design consists of a suspended PDMS membrane sandwiched by top and bottom TiN electrodes with PI as the insulation and buffering layers. Different from existing DEAs, the design in this thesis can induce out-of-plane motion. The functionality was proved initially by COMSOL Multiphysics simulations. Estimations of the effective Young's modulus of the PDMS membrane sandwiched between electrodes and convergence issues in buckling problem modelling were discussed.

Several issues were identified and solved during the fabrication process of TiN electrodes on soft substrate (PDMS). Recipes were found to treat PDMS surface with oxygen plasma to improve adhesion between PDMS and PI. PI thin film was then successfully deposited, patterned and cured on top of PDMS. After solving the PR removal problem, TiN was patterned smoothly on the PI-PDMS stack. Etching of PDMS was tested as the last step using a aluminium hard mask. The etching pattern of the TiN electrodes was analyzed and two assumptions were proposed to explain factors influencing the wrinkle formation.

3.9. Outlook

A DEA full device can be fabricated after patterning the top electrodes with two extra main steps (Referring to the flow chart in Appendix A4). First the membrane will be released by deep reactive ion etching (DRIE) from the backside. It is suggested to put alignment marks also on the backside of the wafer at the beginning of the fabrication process to help the better alignment of the DRIE tool. Test wafers should be used to cal-

culate the exact loop number for etching since even with silicon dioxide as the endpoint stopping layer, overetching will lead to the crack of the PDMS membrane. In addition, it is noted that DIRE is not uniform across the wafer. The etch rate is different depending on the area of the opening and the location on the wafer. This should be considered when designing the masks.

The second main step after top electrodes patterning, also the last step for the whole fabrication is to remove the aluminium hard mask. This step has been tested during the fabrication process of this thesis. Figure 3.21 shows one the DEA device after removing the aluminium hard mask. It can be found that the certain areas of the TiN electrodes were cracked and detached from the surface. The reason for the destroyed TiN electrodes is that TiN was deposited on a nonuniform surface which was caused by the PI stress buffering layer. It was observed on the wafer that when there were less circular patterns on the PI layer (smoother surface), the quality of the TiN electrodes was better. When fabricating the new batch of DEA device in future, the surface uniformity should be focused to avoid failure of TiN electrodes in the final step.

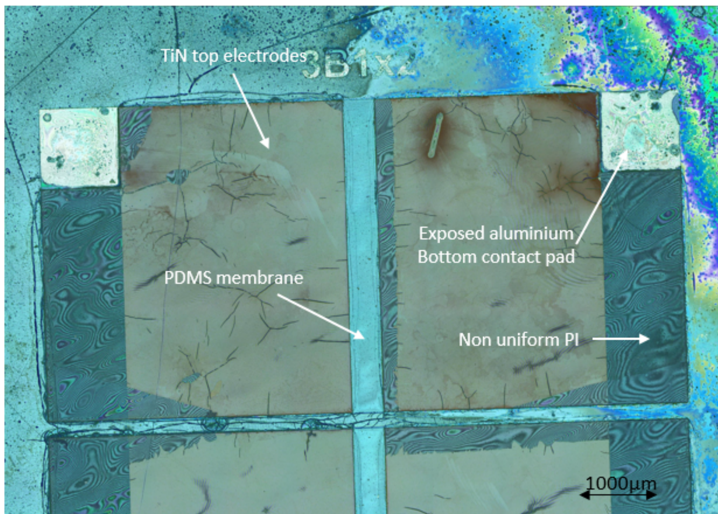

Figure 3.21: DEA after removing aluminium hard mask. Cracks and detached areas can be found on the TiN top electrodes due to the nonuniform surface after deposition

The designed DEA can be characterized statically and dynamically. It suggested to dice the wafer and wire bond the contact pads to certain PCBs which can be connected to high voltage source. First the displacement and strain of the membrane center should be measured when a constant voltage is applied between the electrodes to obtain the relation curve of displacement/strain versus voltage. This step can also test if the insulation is enough or the design need to be modified. Later a square wave at 1Hz should be applied to characterize the response time of the DEA. Finally, the devices should be tested continuously until break to measure the lifetime. The performance and displace-

ment of the membrane can be observed and measuered using white-light interferometer or digital holographic microscope.

Based on the performance during the characterization, the DEA can be further optimized from two perspectives. First, more membrane material with higher dielectric factor can be investigated. It should be mentioned that a cleanroom compatible way of deposition and patterning should be developed before using specific new polymer. The polymer itself should be biocompatible or proper coating should be applied for the cell culture environment. More options of electrodes can be considered and tested for the actuator. The performance of the compliant electrodes should be observed under cell culture environment to compare the select the best option.

After completing the full cycle of further fabrication, characterization and optimization, a DEA that can induce cyclic stretching to cultured cells will be developed.

REFERENCES

[1] P. Brochu and Q. Pei, *Advances in dielectric elastomers for actuators and artificial muscles,* Macromolecular Rapid Communications **31**, 10.

[2] D. Cei, J. Costa, G. Gori, G. Frediani, C. Domenici, F. Carpi, and A. Ahluwalia, *A bioreactor with an electro-responsive elastomeric membrane for mimicking intestinal peristalsis,* Bioinspiration & Biomimetics **12**, 016001 (2017).

[3] A. Poulin, C. S. Demir, S. Rosset, T. V. Petrova, and H. Shea, *Dielectric elastomer actuator for mechanical loading of 2d cell cultures,* Lab on a Chip **16**, 3788 (2016).

[4] S. Akbari and H. R. Shea, *Microfabrication and characterization of an array of dielectric elastomer actuators generating uniaxial strain to stretch individual cells,* Journal of Micromechanics and Microengineering **22**, 045020 (2012).

[5] N. Gaio, B. van Meer, W. Quirós Solano, L. Bergers, A. van de Stolpe, C. Mummery, P. M. Sarro, and R. Dekker, *Cytostretch, an Organ-on-Chip Platform,* Micromachines **7**, 120 (2016).

[6] S. Akbari and H. R. Shea, *An array of 100m×100m dielectric elastomer actuators with 80% strain for tissue engineering applications,* Sensors and Actuators A: Physical Selected Papers presented at Eurosensors XXV, **186**, 236 (2012).

[7] L. Guo, G. S. Guvanasen, X. Liu, C. Tuthill, T. R. Nichols, and S. P. DeWeerth, *A PDMS-Based Integrated Stretchable Microelectrode Array (isMEA) for Neural and Muscular Surface Interfacing,* IEEE Transactions on Biomedical Circuits and Systems **7**, 1 (2013).

[8] S. F. Cogan, *Neural Stimulation and Recording Electrodes,* Annual Review of Biomedical Engineering **10**, 275 (2008).

[9] N. Gaio, *Organ-on-Silicon,* (2019), 10.4233/uuid:ceba7976-a4b0-469e-bdd0-70f0a14dc275.

[10] S. Khoshfetrat Pakazad, *Stretchable micro-electrode arrays for electrophysiology,* (2015).

[11] M. Abadie, *High Performance Polymers - Polyimides Based: From Chemistry to Applications* (BoD – Books on Demand, 2012) google-Books-ID: cOacDwAAQBAJ.

[12] T. Stieglitz, M. Schuetter, and K. P. Koch, *Implantable biomedical microsystems for neural prostheses,* IEEE Engineering in Medicine and Biology Magazine **24**, 58 (2005).

[13] R. Seghir and S. Arscott, *Controlled mud-crack patterning and self-organized cracking of polydimethylsiloxane elastomer surfaces,* Scientific Reports **5**, 14787 (2015).

4

Reflection

TIMELINE COMPARISON

Figure 4.1 is a comparison between the original planned timeline and the actual timeline of this thesis. In general there were two main stages delayed in this thesis. First, the numerical analysis and simulation in COMSOL took longer time than expected. The suspended membrane was designed to buckle when voltage was applied between electrodes. For the buckling problem, COMSOL could not converge in the beginning since it cannot decide the direction of the buckling when the design is symmetric. In order to help COMSOL 'choose' the direction of buckling and slightly disturb the symmetry, a tiny force was applied to the membrane before applying the electric potential. Additional boundary conditions were applied to solve the convergence problem, yet for modelling a buckling situation, it is observed that the problem cannot converge when it is at a switching point of instability between different stable modes. Therefore, even though the performance of the DEA can be simulated in COMSOL, the calculation of displacement versus voltage is not continuous. Modelling this complicated buckling problem took almost two extra months compared to the plan.

The second stage that cost longer time than the plan is the fabrication stage. As discussed in Section 2.5, several issues were identified gradually during the fabrication process. Each critical step on the flowchart had to be tested to find the working recipe since few previous experience available in the ECTM. Another reason is that the status of the equipment and chemicals was unpredictable. Estimation of more time, back-up plans and status checking of chemicals and tools should be considered next time for a better planning.

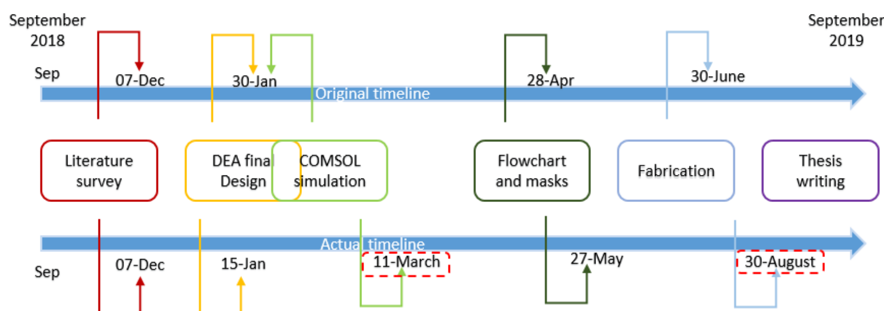

Figure 4.1: Comparison between the original timeline and the actual timeline

FUTURE APPLICATIONS

The initial purpose of designing the DEA in this thesis is to provide an alternative actuation method for Cytostretch that can enable microfluidic system integration. After finishing the fabrication and characterization process, the designed DEA can be integrated with original sensors and PCB boards for Cytostretch. Additional wells or holders for cell culture should be designed to test the performance with actual cells. The membrane surface can be modified with certain topology, for example, micro-pillars to promote better cell adhesion or functionality.

The DEA can be applied in other OOC devices that require cyclic stretching or cyclic mechanical load. As discussed before in Chapter 1, mechanical load is essential for certain types of cells to behave as *in vivo*. The performance of DEA needs to be optimized and tuned respects to different requirements of cells or designs. It is suggested that more investigation should be made focusing on pre-stress of the membrane for better control of tuning the displacement and strain. Having the advantages of being a compact bio-compatible, microscale design, DEAs have a promising possibility to be applied in different OOC platforms.

The fabrication process for depositing and patterning electrodes on soft substrate can have more applications in future. Not only for actuators, the electrodes on top of membrane can be used for sensor fabrication and surface topology regulation. It should be mentioned that more material selection and testings should be made to solve the problem of high impedance and wrinkles at the corner. Successful patterning metals on soft substrate reveals the possibility of fabricating various stretchable electrodes using conventional cleanroom compatible methods that can be adapted into industry scale fabrication very soon.

Experience and lessons learned

Doing my master thesis is the first time I have done a whole project individually from proposing topic in the very beginning till fabrication in the end. I gained valuable experience in project management, engineering design, simulations, cleanroom fabrication and soft skills in presentation and communication. It is important to note down several lessons I learned that could be useful for my projects in future.

Prepare for the unexpected. First lesson is that more time should be planned for solving unexpected situations during project planning. I did not expect and even think about it in the beginning that many things can go wrong and out of my control. It could be as small as the recipes do not work in one specific step or a machine is down for weeks. When fabrication is involved, especially fabricating devices using a new method or with few available experience, leaving more time for the unexpected in the planning is crucial since it is very rare a step or recipe can be defined in the first trial.

Always have a plan B. A lot of unexpected issues can eventually lead to an awkward situation that the project cannot be completely finished in the given time and tool availability. This is where exactly plan B is needed. Sometimes one plan B is not enough or the plan B should be flexible enough. Multiple factors should be considered such as alternative tools for fabrication, a different design for similar performance, extra spare materials, testing structures and tolerance of the design.

Learn from the failure. I have met a lot of failures during my thesis that I lose the count already. It is sad indeed but all the failed experiments, testings and results could be also useful. Finding the reason and doing 'forensic checking' helped me many times to figure out the physics behind, get a new understanding from a different perspective and eventually develop a working recipe. I have to admit that I cried a few times when something is not working as designed. Always being happy is not realistic but what I can do is to take it easy the next day, learn from the failure and continue my work.

A PERSONAL REFECTION

Standing at the ending point of my thesis and looking back, the first phrase comes up to my mind is ’growing up’. One year time can be short but also long. It is too short for me to achieve everything I planned to a satisfied (for me at least) level. Yet it is also long that when I think about the ’me’ one year before, I feel as if I were a different person.

I use the phrase ’growing up’ not only because I gained a lot of knowledge in polymer-based MEMS, or valuable experience in the cleanroom, or precious suggestions and guidance from supervisors and friends. For sure those were important, but the most important thing is, I gradually know a bit what kind of person I am (I can’t say I know entirely still), and what kind of things I want.

I found out I am braver, more determined, or even stubborn than I thought.

I found out reaching out for people is not that hard. It is ok to ask for help.

I found out I am a naive person in many ways but I still don’t think this is a bad thing.

There is a phrase to describe time flies quickly in Chinese called ’GuanQiLanKe’. I think the story behind this phrase is very romantic. It says one day a woodcutter bumped into two people playing Go game in the deep forest. He thought it weird but the Go game was played so well that the woodcutter stopped and started to watch. After one round, one of the players reminded the woodcutter that he should go home now. He said yes and suddenly found out the wood handle of his axe was rotten, the blade was rusted and the two players disappeared. The woodcutter went home but surprised to see all his friends were old people now. In the end he realized that he thought he watched one round of Go game, yet actually a hundred years had already passed.

It is the same feeling doing my thesis, or I would rather say, focused and buried myself in my thesis. It is a joy even with tears and before I realized the time as the woodcutter, one year has already passed. Compared to the ’me’ last year, I am very clear that I want to continue in the MEMS direction, explore more, of course meet more challenges, fail and fail again. I don’t like plain. I like things being complicated, tough and unpredictable.

Home is behind, the world ahead. I know I still have a long way to go and I will go with a smile. I like my one year of doing thesis, same as I like my books, my ukulele and my acrylic paint.

A

APPENDIX A

A.1. Basic Principles of Polymer-Based Actuator Design

A.1.1. Thermal-responsive hydrogels

Principle
The basic principle of the thermal-responsive hydrogel is thermal expansion. No chemical response is involved in the process discussed in this section. Different shape and 3D structure of the hydrogel can be designed to achieve desired deformation.
Application
FigureA.1 [1] presents a thermal-responsive cell stretching device [1]. A thin layer of hydrogel is applied to a patterned substrate to form creases. When the creases deform in depth, the flat material nearby undergoes a deformation to stretch the cells. Cells in an array of $70\mu m \times 90\mu m$ were patterned on the hydrogel at room temperature (22^oC) and reduced roughly to $70\mu m \times 70\mu m$ at 37^oC. A maximum strain of 20% was achieved.

A

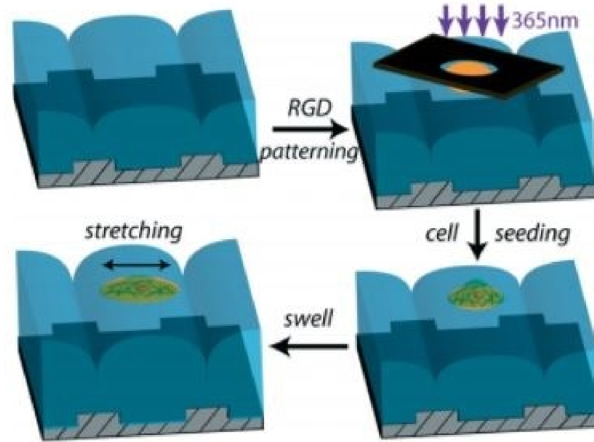

Figure A.1: A dynamic cell stretcher using temperature-responsive hydrogels with patterned surface creases [1].

Advantages
Advantages of thermal-responsive hydrogel can be summarized into following points

- Can have flexible crease patterns in one device:

By changing the geometry of the substrate and crease, multiple strain states of cultured cells on a single substrate can be achieved. This feature can be used to study the correlation between stress distribution and different signal pathways [1].

- Not sensitive to substrate or hydrogel material:

In principle, any bio-compatible hydrogel could be the candidate to design a dynamic thermal responsive cell stretching surface, as long as the coefficient of thermal expansion is within certain range.

- Can be fabricated easily:

The design of this type of OOCs is relatively simple, with no multiple layers of polymers or difficult 3D structures. Therefore, it is not time or process consuming to fabricate.

limitations
One of the most critical problems of using thermal responsive hydrogel is the slow response time (time scale for one-dimensional swelling is around 200s [1]). Using less volume of hydrogel may shorten this time, yet no available data was found during the literature study. Apart from the slow response time, seeding cells in a pattern and at precise locations require an extra photopatterning process. Cells could be misaligned or cluster together.

A.1.2. MAGNETIC ACTUATED DYNAMIC SURFACES

Principle

Magnetic actuated dynamic surfaces are patterned polymer surfaces with embedded metal particles. For the applications that will be discussed in this section, magnetic pillars are created on the PDMS (FigureA.2 [2], FigureA.4 [3]). Cells are cultured on top of the pillars. In a magnetic field, pillars with magnetic particles will bend and apply an external force to cells. Nonmagnetic pillars will deflect in response to the cell behaviour. Therefore the displacement of the nonmagnetic pillars can be used for simultaneous measurement or control group when the cells are actuated by magnetic pillars.

Applications

Figure A.2 [2] and Figure A.3 [2] show a magnetic responsive surface to stretch mouse fibroblasts [2]. Co nanowires were embedded at random locations during the casting process of PDMS. The locations of magnetic pillars were later found and marked under the microscope. A electromagnet is mounted on the microscope stage to apply the magnetic field. To test the dynamics in force application, multiple actuations were applied to cells within 10 min (2 min active field and 2 min intervals with no field). Cells being actuated behaved an increase in local focal adhesion at the point of the magnetic pillars [2].

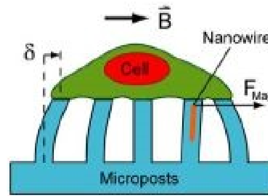

Figure A.2: schematic explanation of a magnetic actuated surface with embedded Co nanowires [2].

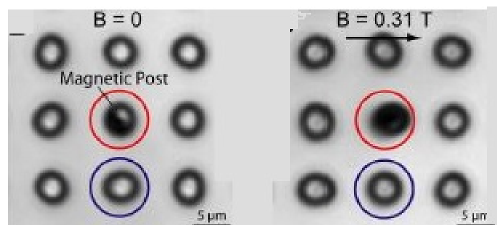

Figure A.3: Bending of a magnetic pillar (red circle) under magnetic field at 0.31T. Nonmagnetic pillar in blue circle for comparison [2].

Figure A.4 [3] is a similar design using magnetic pillars as microactuators. A chip is divided into nine regions with or without magnetic pillars to study the migration of cells. Human endothelial cells were actuated for 48 hrs at 1Hz. The maximum strain measured is 5%.

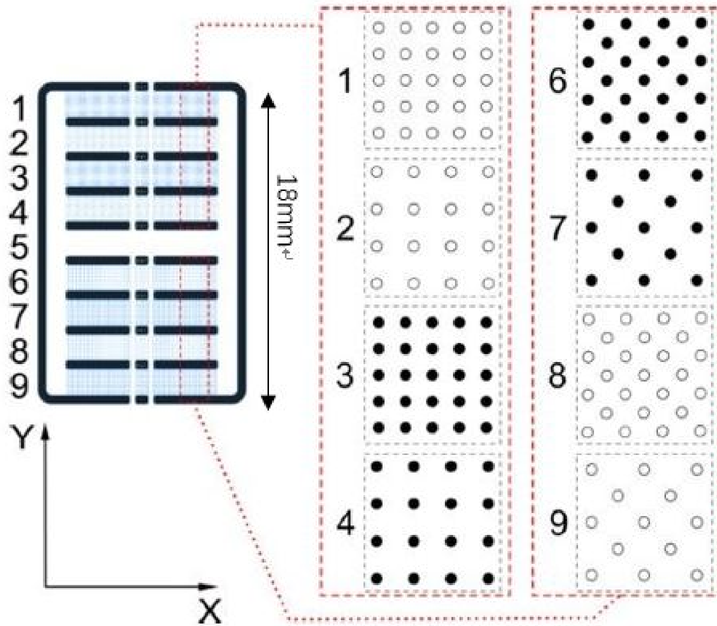

Figure A.4: Cell migration chip with nine regions [3]. Black dots indicate the area with magnetic pillars. Region 5 has no pillars.

Advantages

Magnetic actuated dynamic surfaces have two specific advantages:

- Allow actuation and simultaneous sensing:

As explained in the beginning, the bending of pillars without magnetic particles can be measured to indicate the value and direction of the applied force.

- Allow spatial control of the force:

The direction of the strain can be changed easily by changing the direction of the magnetic field. Therefore, no special geometry or patterns are needed in the device to have uniaxial force. Observing cellular behaviour under forces in different directions at certain periods is also possible by using magnetic actuated micropillars.

Limitations

Existing problems of magnetic actuated dynamic surfaces are listed below:

- The location of the magnetic particles cannot be precisely controlled during fabrication.
- The maximum strain found during literature study (5%) is not sufficient enough for OOCs.
- Long term influences of magnetic fields on cells are yet unknown.

A.1.3. MECHANICAL ACTUATORS

Principle

Mechanical actuators used for OOCs mainly stretch the whole cell culture platform. Since external motors and controllers are inevitable for this method, it is eliminated from the beginning to become a candidate solution for the thesis project. Among designs reviewed during the literature study [4–6], two of them will be explained briefly.

Applications

Figure A.5 [4] presents a device using Shape Memory Alloy (SMA) to stretch a platform for cell culture. SMA is a kind of smart material that 'remembers' its shape at two different temperatures. The shape of SMA can be switched from two states by altering the temperature. In the design below, circuits are connected to a SMA coil (minimum length=22mm) to control the heating of the coil. The SMA coil push or pull the cell culture platform to apply mechanical loads on cells. Although a cooling fan is designed to enable faster cyclic stretching, the minimum cycle time is 4s [4] with the strain within 5% to 30%.

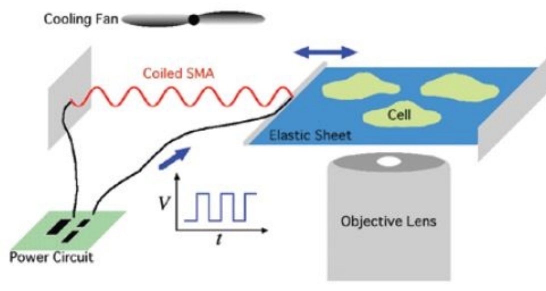

Figure A.5: Stretching an elastic sheet using shape memory alloy [4].

Another design uses piezoelectric actuators to stretch cells in reservoirs [5]. As shown in Figure A.6 [5], pins from the actuator (Braille display) push upwards the PDMS membrane from the back to generate strain. The strain is dependent on the thickness of the PDMS membrane and the frequency of the cyclic stretching can be up to 5Hz [5].

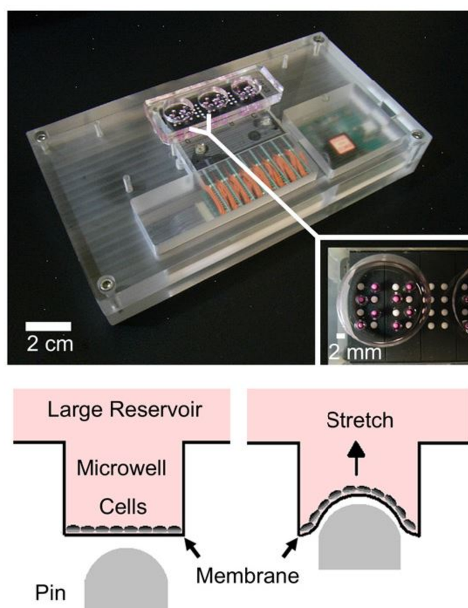

Figure A.6: Display of microwells and schematic graph of a piezoelectrically actuated pin pushing a PDMS membrane in a reservoir [5].

A.1.4. Photothermal actuators

Several types of photosensitive materials were reviewed in the literature [7]. However, most of the photosensitive materials cannot have reversible change of structure. This is mainly because of the irreversible cross-linking of materials initiated by light. However, scholars have been using carbon-based nanomaterials to design microactuators that use light as the stimuli. Carbon materials (carbon nanotubes, graphene, graphite and amorphous carbon) can absorb photon energy and then excite its electrons. The energy of the excited electrons is then transformed into heat [8]. When embedded into polymers as a solo layer or as nanofillers, carbon materials can act as the thermal energy source to actuate the whole structure. Although there are examples of soft robots using carbon-based photothermal actuators [8], no applications for OOCs were found during the literature study. One possible reason could be that cell culture environment has strict requirements of the temperature. Yet the temperature range for existing functional carbon-based photothermal actuators is far beyond the range that cell can survive.

A.1.5. Chemical sensitive dynamic hydrogels

Similar to photosensitive materials, most of the chemical sensitive materials cannot have reversible change of structure due to the irreversible crosslinking. However, a salt stimulated reversible hydrogel were synthesized to regulate the extracellular matrix (ECM) of cells [9]. This hydrogel has two components. One component (collagen) acts as a stable structure and the other component (alginate) has reversible crosslinks (FigureA.7[9]). When alginate was crosslinked, cells were inhibited to move. The mobility was regained

when alginate was uncrosslinked [9].

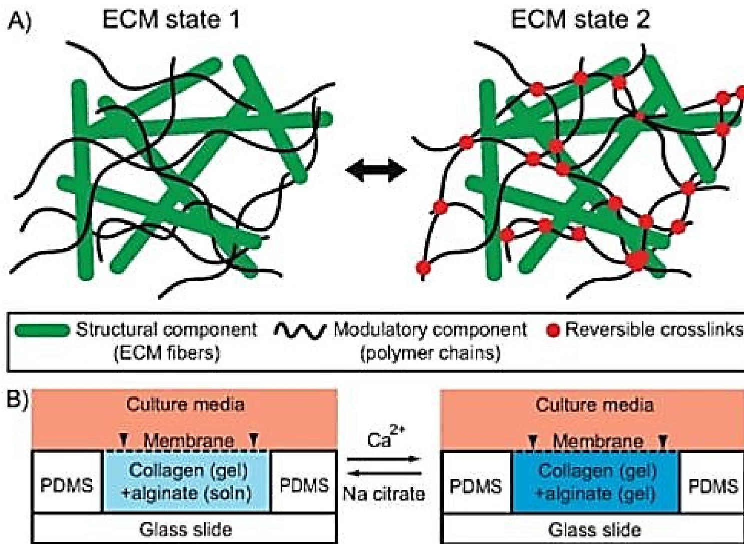

Figure A.7: Schematic diagram of the structure of the hydrogel [9]

Although chemical sensitive dynamic hydrogels can be applied to modify the ECM, no application in tissue or organ level was found. The response time of the hydrogel can be hours which is too slow for actuating cells. In addition, how to control the direction of deformation is still a problem to be solved before integrating this method into OOCs.

A

A.2. CONCEPT EVALUATION FORMS

principle	devices	material	level	cell type	strain/displacement	frequency	optical property	fabrication
electrical	Dielectric elastomer actuators	silicone elastomer/polyurethanes /acrylic elastomer	single/multi cell & monolayer	various	0.1 achieved(uniaxial), 0.3 possible	0.1Hz (achieved)-5Hz (possible)	transparent	Ion implantation is assumed to create the electrodes. Metals such as gold/silver is used (contamination)
electrical	Electro-responsive Hydrogels	syntheic anionic gel	not applicable	not applicable	around 0.5mm for tip of a hydrogel bar	slow (no actual data)	transparent	
thermal	Creased hydrogels	A huge group of chemicals to create hydrogel	single/multi cells	myoblast	0,2	cycle time=200s	transparent hydrogel, opaque substrate	The adhesion chemicals require photopatterning
magnetic	Magnetic microposts/ pillars	PDMS with embedded magnatic particles	single/multi cells	various	0,05	1Hz possible	not transparent	Co & Cu is invloved in the fabrication process
mechanical	Piezoelectrically actuated pins	PDMS+ Piezoelectrically actuated pins	1000 cells/microwell	dermal microvascular endothelial	0.1 (achieved) dependent on PDMS thickness	0.2-5Hz (achieved)	device is transparent, yet the pins are at the bottom, so still not possible for inverted optical microscope	easy to fabricate
mechanical	Shape Memory Alloy (SMA)	SMA coil+circuit+cooling fan	multi cells	dictyostelium cells	500nm-1um	not tested	not transparent	
chemical	Dynamic Hydrogels	Fibrous collagen for stable structure + alginate which gels (Ca+)	single cell	myoblast	not applicable	2 hours achieved	transparent	
optical	photothermal actuators	Carbon based material + polymer	not applicable	not applicable	not applicable	not applicable	not transparent	

Figure A.8: Performances summary

principle	strain/displacement	frequency	biocompatible	optical property	Strain direction	External devices	fabrication
Specifications	>10%	0.1-5Hz	biocompatible	transparent	uniaxial	no	1-10(easy - complicated)
Electrical (DEA)							6
Electrical (hydrogel)							5
Thermal							3
Magnetic							5
Mechanical							1
Chemical	?						5
Optical	good performance in soft robots	?	High temperature				3

Figure A.9: Evaluations. Red=cannot achieve this requirement; Green=Satisfy this requirement; Yellow=need extra modification to meet the requirement or information not avaliable.

A

A.3. LUMPED PDMS MODEL CALCULATION

Figure A.10 left represents the original structure of the complex stack of the PDMS membrane sandwiched between electrodes. In order to calculate the effective Young's modulus of the whole structure, it is simplified into three layers of PDMS, TiN and PI as shown in Figure A.10 right.

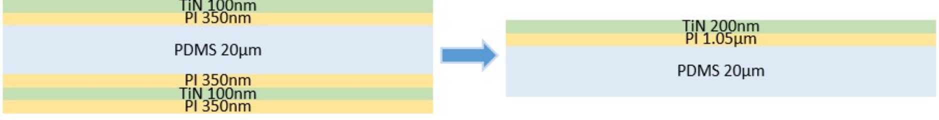

Figure A.10: Left: the original pile of PDMS, TiN and PI stack. Right: equivalent PDMS, TiN and PI stack for lumped Young's modulus calculation

Assume that the original length of the material is $1000\mu m$, the change of length is $10\mu m$ ($L = 1000, dl = 10$). The width of the material w is $1\mu m$. The Young's modulus of the polymers are: PDMS 0.866 MPa as measured; PI 1GPa [10]. The Young's modulus of TiN thin film is yet hard to define since the value depends on the fabrication process, thickness and its landing substrate. It is suggested to measure the Young's modulus of TiN through tensile test to obtain a precise value. In this estimation, the influence of TiN is however neglected considering its very thin thickness. Using equation 3.1, the total force required to cause the change of length is calculated:

$$
\begin{aligned}
F_{total} &= F_{PDMS} + F_{PI} \\
&= E_{PDMS}\frac{dl}{L}A_{PDMS} + E_{PI}\frac{dl}{L}A_{PI} \\
&= \frac{dl}{L}(E_{PDMS}A_{PDMS} + E_{PI}A_{PI}) \\
&= 0.01 \times w \times 10^{-6}(20 \times 10^{-6}E_{PDMS} + 1.05 \times 10^{-6}E_{PI}) \\
&= 0.01 \times w \times 10^{-12}(20E_{PDMS} + 1.05E_{PI})
\end{aligned}
$$

The effective modulus thus will be:

$$
\begin{aligned}
E_{effective} &= \frac{\frac{F_{total}}{A_{total}}}{\frac{dl}{L}} \\
&= \frac{\frac{F_{total}}{21.05 \times w \times 10^{-12}}}{0.01} \\
&= \frac{20E_{PDMS} + 1.05E_{PI}}{21.05} \\
&= 50.7MPa
\end{aligned}
$$

A.4. FLOWCHART

STARTING MATERIAL

Type: n
Orientation: <100>
Resistivity: 2-5 Ωcm
Thickness: 425 ± 15 µm
Diameter: 100 mm

Double Polished wafer x 10

■ ***Step 1-10: Alignment marks***

1. CLEANING: HNO3 99% and 69.5%

Clean 10 minutes in fuming nitric acid at ambient temperature. This will dissolve organic materials. Use wet bench "HNO3 99% (Si)" and the carrier with the red dot.
Rinse Rinse in the Quick Dump Rinser with the standard program until the resistivity is 5 MΩ.
Clean 10 minutes in concentrated nitric acid at 110 °C. This will dissolve metal particles. Use wet bench "HNO3 69,5% 110C (Si)" and the carrier with the red dot.
Rinse Rinse in the Quick Dump Rinser with the standard program until the resistivity is 5 MΩ.
Dry Use the Semitool "rinser/dryer" with the standard program, and the white carrier with red dot.

2. COATING

Use the coater station of the EVG120 system to coat the wafers with photoresist. The process consists of:

- a treatment with HMDS (hexamethyldisilazane) vapor, with nitrogen as a carrier gas
- spin coating of Shipley SPR3012 positive resist, dispensed by a pump
- a soft bake at 95 °C for 90 seconds
- an automatic edge bead removal with a solvent

Always check the relative humidity (48 ± 2 %) in the room before coating, and follow the instructions for this equipment.

Use program "Co - 3012 – zero layer ". No residue allowed on the back.

3. ALIGNMENT AND EXPOSURE

Processing will be performed on the ASML PAS5500/80 automatic wafer stepper.
Follow the operating instructions from the manual when using this machine.
Expose masks COMURK and FWAM with wafer with job "ZEFWAM" with the correct exposure energy: 150mJ
This results in alignment markers for the stepper and contact aligner for wafers.

4. DEVELOPING

Use the developer station of the EVG120 system to develop the wafers. The process consists of:

- a post-exposure bake at 115 °C for 90 seconds
- developing with Shipley MF322 with a single puddle process
- a hard bake at 100 °C for 90 seconds Always follow the instructions for this equipment.

Use program "*Dev - SP*".

A

5. INSPECTION: Linewidth and overlay

Visually inspect the wafers through a microscope and check the line width. No resist residues are allowed in the exposed areas.

6. WAFER NUMBERING

Note down wafer No. in the record sheet.

7. PLASMA ETCHING: Alignment markers (URK's) in Silicon

Use the Trikon Ωmega 201 plasma etcher.
Follow the operating instructions from the manual when using this machine.
It is not allowed to change the process conditions and times from the etch recipe!

Use sequence URK_NPD (with a platen temperature of 20 °C) to etch 120 nm deep ASM URK's into the Si.

8. LAYER STRIPPING: Photoresist

Strip resist Use the Tepla Plasma 300 system to remove the photoresist in an oxygen plasma.
Follow the instructions specified for the Tepla stripper and use the quartz carrier.
Use program 1: 1000 watts power and automatic endpoint detection + 2 min. overetching.

9. CLEANING: HNO3 99% and 69.5%

Clean	10 minutes in fuming nitric acid at ambient temperature. This will dissolve organic materials. Use wet bench "HNO3 99% (Si)" and the carrier with the red dot.
Rinse	Rinse in the Quick Dump Rinser with the standard program until the resistivity is 5 MΩ.
Clean	10 minutes in concentrated nitric acid at 110 °C. This will dissolve metal particles. Use wet bench "HNO3 69,5% 110C (Si)" and the carrier with the red dot.
Rinse	Rinse in the Quick Dump Rinser with the standard program until the resistivity is 5 MΩ.
Dry	Use the Semitool "rinser/dryer" with the standard program.

■ ***Step: 10-13 Silicon oxide on both sides***

10. PECVD DEPOSITION: 1000 nm Silicon oxide

Use the Novellus Concept One PECVD reactor.
Follow the operating instructions from the manual when using this machine.
Use macro OXIDE program: xxxstdSiO2 to deposit a 1000 nm thick SiO2 layer.
Change time to get the right thickness. (ca. 16 s / station)

Note: The deposition time is subject to minor changes, in order to obtain the correct film thickness, check the logbook close to Novellus.

11. MEASUREMENT: Silicon oxide thickness

Use the Leitz MPV-SP measurement system for layer thickness measurements.

Program: Th_SiO2_onSi ; >50nm
Front side Oxide thickness: on a process wafer
Expected thickness: 1000 nm

12. PECVD DEPOSITION: 5000 nm Silicon oxide (BACK)

Use the Novellus Concept One PECVD reactor.
Follow the operating instructions from the manual when using this machine.
Use macro OXIDE program: xxxstdSiO2 to deposit a 5000 nm thick SiO2 layer.

13. MEASUREMENT: Silicon oxide thickness

Use the Leitz MPV-SP measurement system for layer thickness measurements.

Program: Th_SiO2_onSi ; >50nm
Back side Oxide thickness: on a process wafer
Expected Thickness: 5000nm

■ *Step 14-20 Etching back to define membrane area, Mask #1*

14. COATING (BACK)

Use the coater station of the EVG120 system to coat the wafers with photoresist. The process consists of:

- a treatment with HMDS (hexamethyldisilazane) vapor, with nitrogen as a carrier gas
- spin coating of Shipley SPR3027 positive resist, dispensed by a pump
- a soft bake at 95 °C for 90 seconds

Always check the relative humidity (48 ± 2 %) in the room before coating, and follow the instruction for this equipment.
Use program "Co –3027 3µm - no EBR". There will be no edge bead removal. Check backside. No residue are allowed

15. ALIGNMENT AND EXPOSURE (BACK)

Processing will be performed on the contact aligner. Exposure energy: 500mJ
Expose masks_____

16. DEVELOPING (BACK)

Use the developer station of the EVG120 system to develop the wafers. The process consists of:

- a post-exposure bake at 115 °C for 90 seconds
- developing with Shipley MF322 with a double puddle process
- a hard bake at 100 °C for 90 seconds Always follow the instructions for this equipment.

Use program "Dev – SP"

17. INSPECTION: Linewidth and overlay

18. PLASMA ETCHING: Open 5000 nm PECVD SiO2 (BACK)

Use the Drytek Triode 384T plasma etcher.
It is not allowed to change the process conditions from the etch recipe, except for the etch times!
Use recipe STDOXIDE to etch 5000nm oxide and land in the Oxide layer. (ca. 10 mins)

19. LAYER STRIPPING: Photoresist

Strip resist Use the Tepla Plasma 300 system to remove the photoresist in an oxygen plasma.
Use program 1: 1000 watts power and automatic endpoint detection + 2 min. overetching

A

20. CLEANING: HNO3 99% and 69.5%

Clean 10 minutes in fuming nitric acid at ambient temperature. This will dissolve organic materials. Use wet bench "HNO3 99% (Si)" and the carrier with the red dot.
Rinse Rinse in the Quick Dump Rinser with the standard program until the resistivity is 5 MΩ.
Clean 10 minutes in concentrated nitric acid at 110 °C. This will dissolve metal particles. Use wet bench "HNO3 69,5% 110C (Si)" and the carrier with the red dot.
Rinse Rinse in the Quick Dump Rinser with the standard program until the resistivity is 5 MΩ.
Dry Use the Semitool "rinser/dryer" with the standard program, and the white carrier with red dot.

■ *Step 21-27 Create Al bottom contact pad, Mask #2*

21. METALLIZATION: 1500nm AlSi (with 1% Si) @ 350° C

Use the TRIKON SIGMA 204 sputter coater for the deposition of an aluminum metal layer on the wafers. The target must exist of 99% Al and 1% Si, and deposition must be done at 350 °C with an Ar flow of 100 sccm.
Follow the operating instructions from the manual when using this machine.

Use recipe AlSi 1500nm_350C.
Visual inspection: the metal layer must look shiny.

22. COATING

Use the coater station of the EVG120 system to coat the wafers with photoresist. The process consists of:

- a treatment with HMDS (hexamethyldisilazane) vapor, with nitrogen as a carrier gas
- spin coating of Shipley SPR3012 positive resist, dispensed by a pump
- a soft bake at 95 °C for 90 seconds
- an automatic edge bead removal with a solvent

Always check the relative humidity (48 ± 2 %) in the room before coating, and follow the instructions for this equipment.
Use program "Co - 3012 – 1.4um". No residue allowed on the back.

23. ALIGNMENT AND EXPOSURE

Processing will be performed on the Contact Aligner using Mask___, Exposure energy 150mJ

24. DEVELOPING

Use the developer station of the EVG120 system to develop the wafers. The process consists of:

- a post-exposure bake at 115 °C for 90 seconds
- developing with Shipley MF322 with a single puddle process
- a hard bake at 100 °C for 90 seconds Always follow the instructions for this equipment.

Use program "*Dev - SP*".

25. WET ETCHING AlSi : PES 35 °C

Etch Use dedicated wet bench PES at temperature 35° C.
The bath contains PES solution.
Time Until all AL is removed. Time TBD (around 9 mins)
QDR Rinse in the Quick Dump Rinser with the standard program.
Etch Use dedicated wet bench Poly-Si etch
Time Until all Si residue is removed. Time TBD (around 30 s)

QDR Rinse in the Quick Dump Rinser with the standard program.
Dry Use the manual dryer.

26. LAYER STRIPPING: Photoresist

Strip Use dedicated wet bench Acetone 40 °C

27. CLEANING: HNO3 99% (METAL)

Clean 10 minutes in fuming nitric acid at ambient temperature. This will dissolve organic materials. Use wet bench "HNO3 99% (metal)" and the carrier with a red and yellow dot.
Rinse Rinse in the Quick Dump Rinser with the standard program until the resistivity is 5 MΩ.
Dry Use the Semitool "rinser/dryer" with the standard program, and the white carrier with a black dot.

- *Step 28-34 Polyimide deposition to isolate electrodes from the bottom. 2 wafers will jump this process for future testing. Mask #3*

POLYIMIDE NOTE: SHOULD BE FINISHED IN A HALF DAY

28. MANUAL COATING

Use the Brewer Science manual coater system to coat the wafers with Polyimide LTC 9305.
The process consists of:

- Use the membrane chuck for non-contaminated wafers
- spin coating 800nm? of Fujifilm LTC9305 negative polyimide, dispensed by a manual syringe

Use program "no 30: 60sec at 6000RPM". (recipe needs to be checked)

29. MANUAL BAKING STEP

Use the hotplate of manual coater system to soft bake the wafers with Polyimide LTC 9305.
The process consists of:
Bake 120 s @ 100C

30. INSPECTION AND CLEANING

Visually inspect the back side of the wafers and clean with acetone.
Also clean the edge of the wafer with a Q-tip with HTRD2 developer.
No polyimide residues are allowed.

31. ALIGNMENT AND EXPOSURE

Processing will be performed on the contact aligner. Exposure energy: 120mJ
Use the transport wafer for clean wafers:
Develop the transport wafer also in HTRD2

32. POST EXPOSURE DELAY (PED) OR POST EXPOSURE BAKE (PEB)

PEB: 60s @ 50C

33. DEVELOPING MANUAL

Use the developer red room. Use special glassware for polyimide

- Developing with HTRD2, time 1m15s.
- A hard bake at 100°C for 90 seconds

A

34. FINAL CURE - KOYO

In vacuum and under low N2 flow.
Use dedicated Al carrier plate for clean wafers under the process wafer.
Standard Cure 60 min @ 350 °C

END POLYIMIDE

- *Step 35-41 TiN electrodes deposition and pattern, Mask #4*

35. METALLIZATION: RF etch + Ti 10nm + TiN 100nm @ 25

Use the TRIKON SIGMA 204 sputter coater for the deposition of a TiN metal layer with Ti adhesion layer on the wafers.
The deposition must be done at 25 °C with an Ar flow of 100 sccm. Follow the operating instructions from the manual when using this machine.
Use recipe Ti 10_TiN 100_25C (Check and confirm the low energy recipe before start)

LUR TEST REQUESTED!
Note a TiN in between needs to be done between the process wafers.
Visual inspection: the metal layer must look shiny.

36. COATING

Use the coater station of the EVG120 system to coat the wafers with photoresist. The process consists of:

- a treatment with HMDS (hexamethyldisilazane) vapor, with nitrogen as a carrier gas
- spin coating of Shipley SPR3012 positive resist, dispensed by a pump
- a soft bake at 95 °C for 90 seconds
- an automatic edge bead removal with a solvent

Always check the relative humidity (48 ± 2 %) in the room before coating and follow the instructions for this equipment.
Use program "Co - 3012 – 1.4um - topo". No residue allowed on the back.

37. ALIGNMENT AND EXPOSURE

Processing will be performed on the Contact Aligner. Exposure energy: 150mJ

38. DEVELOPING

Use the developer station of the EVG120 system to develop the wafers. The process consists of:

- a post-exposure bake at 115 °C for 90 seconds
- developing with Shipley MF322 with a double puddle process
- a hard bake at 100 °C for 90 seconds Always follow the instructions for this equipment.

Use program "Dev – SP".

39. INSPECTION: Linewidth and overlay

Visually inspect the wafers through a microscope: No resist residues are allowed in exposed part.

40. PLASMA ETCHING: TiN 100 nm (sputtered at 25 °C)

Use the Trikon Ωmega 201 plasma etcher.
Follow the operating instructions from the manual when using this machine.
It is not allowed to change the process conditions and times from the etch recipe!

Use sequence TiN_NSL Special recipe (with a platen temperature of 25 ºC) to etch the TiN layer with endpoint detection. Landing on Polyimide

41. LAYER STRIPPING: Photoresist

Strip resist Use the Tepla Plasma 300 system to remove the photoresist in an oxygen plasma. Follow the instructions specified for the Tepla stripper and use the quartz carrier.
Use program 2 flash.

■ *Step 42-48 Second layer of Polyimide, 2 wafers jump this process for future testing , Mask #4*

POLYIMIDE IN POLYMER LAB

42. MANUAL COATING

Use the Brewer Science manual coater system to coat the wafers with Polyimide LTC 9305.
The process consists of:

- Use the membrane chuck for non-contaminated wafers
- spin coating of 800nm Fujifilm LTC9305 negative polyimide, dispensed by a manual syringe

Use program "no 30: 60sec at 6000RPM". (recipe needs to be checked)

43. MANUAL BAKING STEP

Use the hotplate of manual coater system to soft bake the wafers with Polyimide LTC 9305.
The process consists of:

Bake 120 s @ 100C

44. INSPECTION AND CLEANING

Visually inspect the back side of the wafers and clean with acetone.
Also clean the edge of the wafer with a Q-tip with HTRD2 developer.
No polyimide residues are allowed.

45. ALIGNMENT AND EXPOSURE

Processing will be performed on the Contact Aligner E=100mJ
Use the transport wafer for clean wafers:
Develop the transport wafer also in HTRD2

46. POST EXPOSURE DELAY (PED) OR POST EXPOSURE BAKE (PEB)

PEB: 60s @ 50C

47. DEVELOPING MANUAL

Use the developer red room. Use special glassware for polyimide

- Developing with HTRD2, time 1m15s.
- A hard bake at 100°C for 90 seconds

Always follow the instructions for this equipment.

48. FINAL CURE KOYO

In vacuum and under low N2 flow.
Use dedicated Al carrier plate for clean wafers under the process wafer.
Standard Cure 60 min @ 350 °C

END POLYIMIDE

A

■ *Step 49-55 Put 20um PDMS on the wafer*

49. OXYGEN TREATMENT (in order to improve adhesion between polyimide and PDMS)

Use ALCATEL

PDMS IN POLYMER LAB

50. PREPARING PDMS

5 wafers with ratio 10:1
5 wafers with ratio 20:1, Note down the wafer number on the table

51. PDMS MIXING AND DEGASING

Use the Thinky Speedmixer for mixing and degasing the PDMS elastomer and curing agent.
Weigh the total mass of the sample holder with the PDMS and adjust the mass in the Speedmixer.
Make sure that the cup holder is properly located in the machine.

52. MANUAL COATING PDMS

Use manual coater system to coat the wafers with PDMS. The process consists of:

- Cover the inside of the coating station with aluminum foil
- Spin coat the PDMS by dispensing it with manual syringe

53. PDMS BAKE

Use the Memmert oven in tunnel 1 to perform an extra resist bake:
bake the wafers at 90 °C for 30 minutes Note: Use a dedicated rack to bake the wafers

END PDMS IN POLYMER LAB

54. INSPECTION PDMS RESIDUES

Visually inspect the wafers through a microscope, and check if the wafers are clean. No resist or PDMS residues are allowed.

55. OXYGEN TREATMENT (in order to improve adhesion between polyimide and PDMS)

Use ALCATEL

■ *Step 56-62 Put third layer of polyimide to promote adhesion for top electrodes, Mask #4*

Polyimide IN POLYMER LAB

56. MANUAL COATING

Use the Brewer Science manual coater system to coat the wafers with Polyimide LTC 9305.
The process consists of:

- Use the membrane chuck for non-contaminated wafers
- spin coating of 800nm Fujifilm LTC9305 negative polyimide, dispensed by a manual syringe

Use program "no 30: 60sec at 6000RPM". (recipe needs to be checked)

57. MANUAL BAKING STEP

Use the hotplate of manual coater system to soft bake the wafers with Polyimide LTC 9305.
The process consists of:
Bake 120 s @ 100C

58. INSPECTION AND CLEANING

Visually inspect the back side of the wafers and clean with acetone.
Also clean the edge of the wafer with a Q-tip with HTRD2 developer.
No polyimide residues are allowed.

59. ALIGNMENT AND EXPOSURE

Processing will be performed on the Contact Aligner. E=100mJ
Follow the operating instructions from the manual when using this machine.
Use the transport wafer for clean wafers:
Develop the transport wafer also in HTRD2

60. POST EXPOSURE DELAY (PED) OR POST EXPOSURE BAKE (PEB)

PEB: 60s @ 50C

61. DEVELOPING MANUAL

Use the developer red room. Use special glassware for polyimide

- Developing with HTRD2, time 1m15s.
- A hard bake at 100°C for 90 seconds

Always follow the instructions for this equipment.

62. FINAL CURE KOYO

In vacuum and under low N2 flow.
Use dedicated Al carrier plate for clean wafers under the process wafer.
Cure @ 200 °C, Time to be defined

END Polyimide

■ *Step 63-69 Put TiN top electrodes, Mask #3*

63. METALLIZATION: RF etch + Ti 10nm + TiN 100nm @ 25

Use the TRIKON SIGMA 204 sputter coater for the deposition of a TiN metal layer with Ti adhesion layer on the wafers.
The deposition must be done at 25 °C with an Ar flow of 100 sccm. Follow the operating instructions from the manual when using this machine.
Use recipe Ti 10_TiN 100_25C. (Check and confirm the low energy recipe before start)

LUR TEST REQUESTED!
Note a TiN in between needs to be done between the process wafers.
Visual inspection: the metal layer must look shiny.

64. COATING

Use the coater station of the EVG120 system to coat the wafers with photoresist. The process consists of:

- a treatment with HMDS (hexamethyldisilazane) vapor, with nitrogen as a carrier gas

A

- spin coating of Shipley SPR3012 positive resist, dispensed by a pump
- a soft bake at 95 °C for 90 seconds
- an automatic edge bead removal with a solvent

Always check the relative humidity (48 ± 2 %) in the room before coating and follow the instructions for this equipment.
Use program "Co - 3012 – 1.4um - topo". No residue allowed on the back.

65. ALIGNMENT AND EXPOSURE

Processing will be performed on the Contact Aligner. E=150mJ

66. DEVELOPING

Use the developer station of the EVG120 system to develop the wafers. The process consists of:

- a post-exposure bake at 115 °C for 90 seconds
- developing with Shipley MF322 with a double puddle process
- a hard bake at 100 °C for 90 seconds Always follow the instructions for this equipment.

Use program "Dev – SP".

67. INSPECTION: Linewidth and overlay

Visually inspect the wafers through a microscope: No resist residues are allowed in exposed part.

68. PLASMA ETCHING: TiN 100 nm (sputtered at 25 °C)

Use the Trikon Ωmega 201 plasma etcher.
Follow the operating instructions from the manual when using this machine.
It is not allowed to change the process conditions and times from the etch recipe!

Use sequence TiN_NSL Special recipe (with a platen temperature of 25 ºC) to etch the TiN layer with endpoint detection. Landing on Polyimide

69. LAYER STRIPPING: Photoresist

Strip resist — Use the Tepla Plasma 300 system to remove the photoresist in an oxygen plasma. Follow the instructions specified for the Tepla stripper and use the quartz carrier.
Use program 2 flash.

- *Step 70- 76 Put Al hard mask and etch PDMS Mask #5*

70. METALLIZATION: 250nm Al pure @ RT or 250nm Al/Si @ RT

Use the TRIKON SIGMA 204 sputter coater for the deposition of an AL metal layer on the wafers. The target must exist of 99% Al and 1% Si And Ti, and deposition must be done at RT with an Ar flow of 100 sccm. Follow the operating instructions from the manual when using this machine.
Use recipe Al 250nm_RT.

LUR TEST required!
Visual inspection: The metal layer is not very shiny.

71. COATING

Use the coater station of the EVG120 system to coat the wafers with photoresist. The process consists of:

- a treatment with HMDS (hexamethyldisilazane) vapor, with nitrogen as a carrier gas
- spin coating of AZ9260 positive resist, dispensed by syringe

- a soft bake at 95 °C for 90 seconds
- no edge bead removal

Always check the relative humidity (48 ± 2 %) in the room before coating, and follow the instructions for this equipment.
Use program "1_AZ9260-8um ". No residue allowed on the back.
Wait for 30 mins after coating

~~72. SOFT BAKE~~

~~Bake in memmert the wafers for 30 minutes at 80 degrees C.~~
~~Handle carefully.~~

73. ALIGNMENT AND EXPOSURE

Processing will be performed on the contact aligners.
Follow the operating instructions from the manual when using this machine.
Expose wafer with the correct exposure energy: **Energy to be defined**
Wait for 30mins after exposure

74. DEVELOPMENT

Develop manually.
See the instruction in CR100
Use AZ400K with ratio AZ400K:H2O=1:2

75. PLASMA ETCHING: AlSi 250 nm

Use the Trikon Ωmega 201 plasma etcher.
Follow the operating instructions from the manual when using this machine.
It is not allowed to change the process conditions and times from the etch recipe!

Use the sequence with a platen temperature of 25 ºC) to etch the AlSi layer with endpoint detection.
Landing on PDMS

76. PLASMA ETCHING: PDMS (here the rest of the photoresist on Al is etched as well)

Use the Trikon Ωmega 201 plasma etcher.
Follow the operating instructions from the manual when using this machine.
It is not allowed to change the process conditions and times from the etch recipe!

Use sequence PDMS_4 (with a platen temperature of 25 ºC) to etch the PDMS layer without endpoint detection.
Landing on Al contact pad

- *Step 77- 86 Backside etching of Si, SiO2, and Al hard mask*

77. PLASMA ETCHING SILICON (BACK)

Use the Rapier Omega i2L plasma etcher. It is not allowed to change the process conditions from the etch recipe. Change only number of cycles.
Follow the operating instructions from the manual when using this machine.
It is not allowed to change the process conditions and times from the etch recipe! (Cross-contamination is avoided with Ti barrier layer.)
LANDING on SiO2

A

Use the sequence with a platen temperature of 20 °C to etch the Si layer and stop on SiO2. Ca. 500 cycles. Etching program includes end-point detection.

78. MANUAL COATING PHOTORESIST

Use manual coater system to coat the wafers with photoresist. The process consists of:

- Spin coat the Shipley SPR3027 positive resist by dispensing it with manual syringe
- Use the Non-vacuum edge-chuck
- Make sure the edge of the wafer is completely covered with resist.

79. MANUAL BAKING STEP

Use the Memmert oven in tunnel 1 to perform an extra resist bake:
bake the wafers at 100 °C for 15-30min minutes
Note: Use a dedicated rack to bake the wafers

80. WET ETCHING BHF (PDMS): Etch 2um PECVD SiO2 SAL

Etch Use dedicated wet bench BHF 1:7 at ambient temperature, and the carrier with the 2 blue dots.
The bath contains a buffered HF solution.
Change the BHF solution to prevent cross-contamination
Time Until all oxide is removed. Time TBD (around 30 minutes)
Rinse Rinse in the water for 5 minutes.
Dry Use the manual dryer.

81. RESIST LAYER STRIPPING: ACETONE SAL

Use special beaker, wafer holder and rinse bath for this step
Strip resist Use acetone at RT to remove the resist for 2 min.
No resist residues are allowed. Rinse in water
Manual drying.

82. MANUAL COATING PHOTORESIST

Use manual coater system to coat the wafers with photoresist. The process consists of:

- Spin coat the Shipley SPR3027 positive resist by dispensing it with manual syringe
- Use the Non-vacuum edge-chuck
- Make sure the edge of the wafer is completely covered with resist.

83. ALIGNMENT AND EXPOSURE

Processing will be performed on the contact aligners.
Follow the operating instructions from the manual when using this machine.
Expose wafer with the correct exposure energy:

84. DEVELOPMENT

The process consists of:

- development step using Shipley MF322developer (single puddle process)
- hard bake at 100°C for 1.5 min.

Develop manually.

85. WET ETCHING PES: 250 nm Al

Etch	Use dedicated wet bench PES. The bath contains PES solution.
Time	Until all AL is removed. Time TBD (around 5 mins)
Rinse	Rinse in the water for 5 minutes.
Dry	Use the manual dryer.

86. RESIST LAYER STRIPPING: ACETONE SAL

Use special beaker, wafer holder and rinse bath for this step

Strip resist	Use acetone at RT to remove the resist for 2 min. No resist residues are allowed. Rinse in water Manual drying.

Poly-2
PDMS
Poly-3
TiN
Poly-4

A.5. PDMS SPIN COATING THICKNESS CONFIGURATION

PDMS 5:1

speed 5000/300/30	time (s)	t1 (um)	t2 (um)	t3 (um)	t4 (um)	t5 (um)	ave (um)	S
	25	14,934	14,966	14,275	14,755	14,213	14,6286	0,360847
	30	13,404	13,416	13,315	13,263	12,979	13,2754	0,177399
	35	12,271	11,764	12,608	11,313	11,797	11,9506	0,499944
	40	11,97	11,361	11,857	12,288	12,039	11,903	0,34172

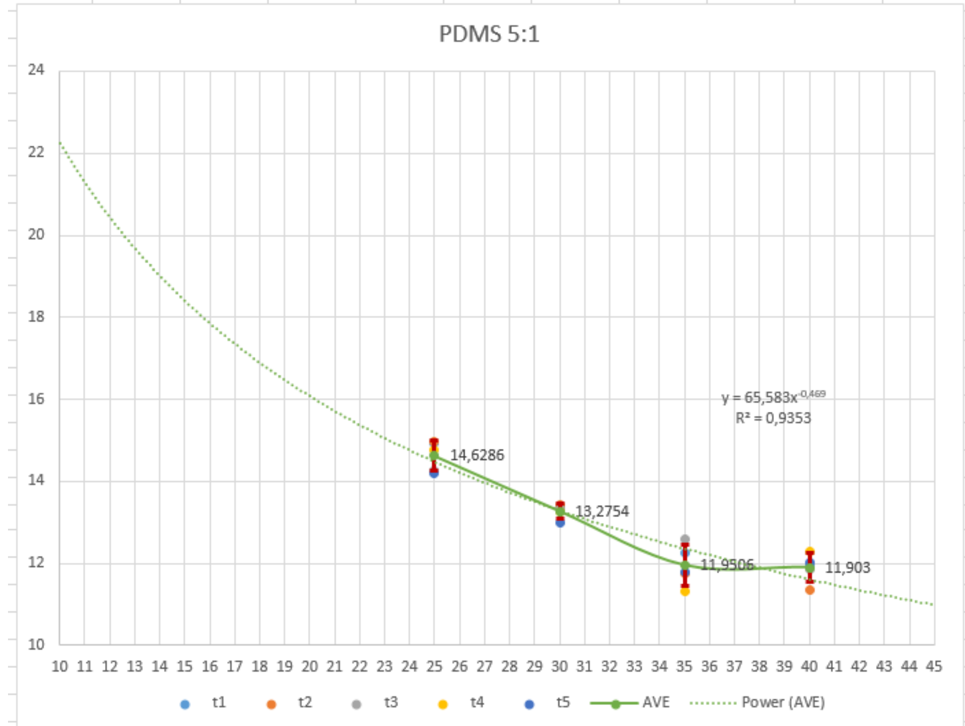

PDMS 20:1

speed 4000/300/30	time (s)	t1 (um)	t2 (um)	t3 (um)	t4 (um)	t5 (um)	ave (um)	
	25	25,453	25,124	25,187	25,015	25,907	25,3372	0,357039
	30	23,078	23,927	22,695	22,984	23,595	23,2558	0,496375
	35	22,187	21,889	21,376	21,901	21,745	21,8196	0,295284
	40	20,566	20,126	19,706	20,491	20,994	20,3766	0,48545

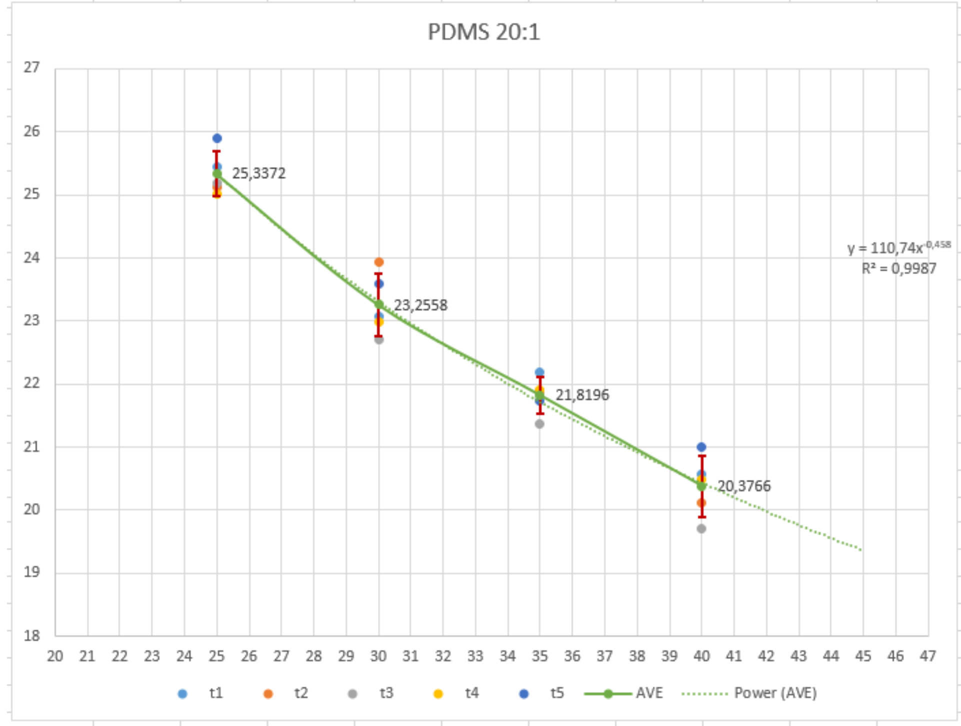

A

A.6. PI KOYO OVEN CURING RECIPE

Document nr. : HMA-KOYO-170118-2
Document : Koyo Oven
Administrator : EKL- SEE- POLAB
Contact info.: SEE (Hitham Mahmoud- Tel. no: 81787)

Page nr. : 1
Programing Scheme for recipes PI curing @ 200°c for 2.5h
Date: / /
Operator name: No.18

20°C
140°C
200°C
200°C
20°C
20°C
2.5h

			1	2	3	4	5	6	7	8	9	10	11	12	13	14	15	16	17	18	19	20
Pattern	1	Temp	0.0	140	140	200	200	200	20	20												
	2	Time	0.5	1.00	0.01	1.30	1.00	0.01	3.00	0.01												
Event 1	1	On																				
	2	Off																				
Event 2	1	On																				
	2	Off																				
Event 3	1	On																				
	2	Off																				
purge Time Event 1	1	On	✓																			
	2	Off		X	X	X	X	X	X	X												
Running valve Time Event 2	1	On		✓	✓	✓	✓	✓	✓	✓												
	2	Off	X																			
cooling valve Time Event 3	1	On						[illegible]	✓	✓												
	2	Off	X	X	X	X	X	X														
cooling blower Time Event 4	1	On						[illegible]	✓	✓												
	2	Off	X	X	X	X	X	X														
sampling Time Event 5	1	On	✓																			
	2	Off	[illegible]	X	X	X	X	X	X	X												
PID set No. (CH1)			1	0	0	0	0	0	0	0												
G. Soak (CH1)			X	X	5	X	5	5	X	5												
G. Soak time out			X	X	X	X	X	X	X	X												
PV start			0	0	0	0	0	0	0	0												
Cycle			0	0	0	0	0	0	0	0												
Pattern Link			0	0	0	0	0	0	0	0												

A

REFERENCES

[1] D. Chen, R. D. Hyldahl, and R. C. Hayward, *Creased hydrogels as active platforms for mechanical deformation of cultured cells,* Lab on a Chip **15**, 1160 (2015).

[2] N. J. Sniadecki, A. Anguelouch, M. T. Yang, C. M. Lamb, Z. Liu, S. B. Kirschner, Y. Liu, D. H. Reich, and C. S. Chen, *Magnetic microposts as an approach to apply forces to living cells,* Proceedings of the National Academy of Sciences **104**, 14553 (2007).

[3] F. Khademolhosseini, C.-C. Liu, C. J. Lim, and M. Chiao, *Magnetically actuated microstructured surfaces can actively modify cell migration behaviour,* Biomedical Microdevices **18**, 13 (2016).

[4] Y. Iwadate and S. Yumura, *Cyclic stretch of the substratum using a shape-memory alloy induces directional migration in Dictyostelium cells,* BioTechniques **47**, 757 (2009).

[5] Y. Kamotani, T. Bersano-Begey, N. Kato, Y.-C. Tung, D. Huh, J. W. Song, and S. Takayama, *Individually programmable cell stretching microwell arrays actuated by a Braille display,* Biomaterials **29**, 2646 (2008).

[6] R. Fior, S. Maggiolino, M. Lazzarino, and O. Sbaizero, *A new transparent Bio-MEMS for uni-axial single cell stretching,* Microsystem Technologies **17**, 1581 (2011).

[7] J. Kim and R. C. Hayward, *Mimicking dynamic in vivo environments with stimuli-responsive materials for cell culture,* Trends in Biotechnology **30**, 426 (2012).

[8] B. Han, Y.-L. Zhang, Q.-D. Chen, and H.-B. Sun, *Carbon-Based Photothermal Actuators,* Advanced Functional Materials **28**, 1802235 (2018).

[9] B. M. Gillette, J. A. Jensen, M. Wang, J. Tchao, and S. K. Sia, *Dynamic Hydrogels: Switching of 3d Microenvironments Using Two-Component Naturally Derived Extracellular Matrices,* Advanced Materials **22**, 686 (2010).

[10] L. Guo, G. S. Guvanasen, X. Liu, C. Tuthill, T. R. Nichols, and S. P. DeWeerth, *A PDMS-Based Integrated Stretchable Microelectrode Array (isMEA) for Neural and Muscular Surface Interfacing,* IEEE Transactions on Biomedical Circuits and Systems **7**, 1 (2013).